Caveolin1 Mediates the Midkine-Induced Angiotensin I Converting Enzyme Signaling in Human Lung Epithelial Cells

by

Jung-Eun Ustina Huh

A thesis submitted in conformity with the requirements
for the degree of Master of Science

Department of Physiology
University of Toronto

Caveolin1 Mediates the Midkine-Induced Angiotensin I Converting Enzyme Signaling in Human Lung Epithelial Cells

Jung-Eun Ustina Huh

Master of Science

Department of Physiology
University of Toronto

2016

Abstract

Introduction: Midkine (MK), a novel cytokine, is upregulated in acute respiratory distress syndrome (ARDS) patients. MK interacts with the cell surface receptor Notch2 to induce epithelial-mesenchymal transition (EMT) through angiotensin I converting enzyme (ACE) in lung epithelial cells. However, it remains unknown how Notch2 modulates ACE expression, since there is lack of direct interaction between these two molecules. Caveolin1 (Cav1) has been shown to regulate ACE expression. We hypothesized that Cav1 interacts with Notch2 to mediate the MK-induced ACE signaling pathway.

Methods: Human lung epithelial cells were used for co-immunoprecipitation to examine Notch2 interaction with Cav1. Cells were stimulated with recombinant human midkine (rhMK) and transfected with Cav1 siRNA to determine the role of Cav1 on Notch2, ACE, and EMT.

Results: Cav1 bound specifically with Notch2, but not Notch1, Notch3, or Notch4. Cav1 knockdown blocked the rhMK- induced ACE and EMT signaling in lung epithelial cells.

Conclusion: Cav1 is required to mediate the MK-Notch2-ACE signaling pathway.

Word count: 150

Acknowledgments

First, I would like to acknowledge my supervisor, **Dr. Haibo Zhang**, for giving me this amazing opportunity and for being a mentor to me for the past two years. Dr. Zhang was always open and enthusiastic towards me when I approached him with questions, not only pertaining to my project, but about anything in general. I was truly inspired by our fruitful discussions on life, family, and career. I am very grateful for all of the professional advice and scientific knowledge he shared with me, which has shaped me to become a good scientist. Most of all, he taught me the importance of optimism, perseverance, and resiliency, and these are traits I will surely take into all of my future endeavors.

I would also like to thank the members of my thesis committee, **Dr. Mingyao Liu** and **Dr. John Laffey**, for the time they invested in discussing and contributing towards my work. I am very grateful for all of the support and intellectual insight they provided for my project. I remember getting nervous prior to my meetings with them, but after every single meeting I was left joyful, thankful, and full of inspiration and motivation to continue my project. I could not have completed my thesis without their continual guidance throughout these past two years.

I also express my gratitude towards **Dr. Bing Han** for the time and energy he spent in teaching me the crucial wet lab techniques for my work. I would like to thank him for always being available to answer my questions. His expertise goes beyond other research associates I have previously worked with.

I would also like to thank **Julie Khang**, who continually encouraged me through all of the difficulties of research and for also providing the administrative and technical support for my project. I am very grateful for her friendship and I really could not have completed my thesis without her support.

I would also like to thank the members of our laboratory- **Manshu Li**, **Diana Islam**, **Alice Grassi**, **Dimitris Toumpanakis**, **Alice Luo**, **Yonghao Xu**, **Qingqing Dai**, and **Junbo Zheng** for their friendship and support through the past two years.

I would like to thank my family- **Mom**, **Dad**, my younger **Sister**, and my **Grandparents**- who have always prayed for me and given me endless encouragement and support. I am extremely grateful to have both parents in academia who are all too familiar with the joys and difficulties of research. Their academic pursuits in Masters and Doctoral programs alone inspire me and push me to keep going. I am also very thankful to my sister Deb, who continually motivates me through her endeavors and accomplishments. I would also like to thank my grandparents for continually praying for me and for supporting me. I could not be where I am today without them.

Lastly, I would like to thank **God** who has given me life and purpose. I truly believe that these past two years were a part of His plan to equip me and prepare me to serve His kingdom. I am excited to see what His plan holds for me in the next chapter of my life.

1 Thessalonians 5:16-18

Contributions

The work presented in this thesis was principally performed by myself, or otherwise stated.

Dr. Bing Han provided guidance with establishing the co-immunoprecipitation protocol in Figure 10.

Julie Khang provided technical assistance for the two-hit stimulation experiment in Figure 7 and the ACE ELISA in Supplementary Figure 4.

Alice Luo provided technical assistance for performing the ACE, Cytokeratin8, and α-SMA Western blots in Figure 13.

Funding was provided by the Canadian Institutes for Health Research to Dr. Haibo Zhang.

Table of Contents

List of Figures

List of Supplementary Figures

List of Abbreviations

ACE	Angiotensin I converting enzyme
AECC	American-European Consensus Conference
ARDS	Acute respiratory distress syndrome
β-actin	Beta-actin
BEAS-2B	Normal human bronchial epithelial cell line
BSA	Bovine serum albumin
Cav1	Caveolin1
CSD	Caveolin scaffolding domain
DMEM	Dulbecco's Modified Eagle Medium
EDTA	Ethlyenediaminetetraacetic acid
ECD	Extracellular domain
EGF	Epidermal growth factor-like
EMT	Epithelial-mesenchymal transition
EndoMT	Endothelial-mesenchymal transition
HCl	Hydrochloric acid
HRP	Horseradish peroxidase
ICD	Intracellular domain
IgG	Immunoglobulin G
IP	Immunoprecipitation
LDH	Lactate dehydrogenase
LNR	Lin-12/Notch repeats

mAb	Monoclonal antibody
MK	Midkine
MV	Mechanical ventilation
OD	Optical density
pAb	Polyclonal antibody
PAGE	Polyacrylamide gel electrophoresis
PaO_2/FiO_2	The ratio of partial pressure arterial oxygen (PaO_2) and fraction of inspired oxygen (FiO_2)
PBS	Phosphate-buffered saline
rhMK	Recombinant human MK
RNA	Ribonucleic acid
scRNA	Scrambled siRNA
SDS	Sodium dodecyl sulfate
siRNA	Small interfering RNA
TAD	Transactivation domain
TBS-T	Tris-buffered saline Tween
VILI	Ventilator-induced lung injury

List of Appendices

Chapter 1
Introduction

OVERVIEW

Acute respiratory distress syndrome (ARDS) is a pathological condition in which direct or indirect insults to the lung induce an acute inflammatory response and tissue injury that may lead to chronic fibrotic development [1, 2]. Mechanical ventilation (MV) serves as the major therapy for life support; however, prolonged use of MV may aggravate lung injury, resulting in ventilator-induced lung injury (VILI). VILI may induce and worsen fibrotic response, leading to high mortality in ARDS patients [3]. Therefore protective ventilation is required whenever and wherever possible, while novel pharmacologic therapeutic approaches are needed in the management of ARDS.

The thesis will begin with an overview of ARDS, including a brief history of ARDS, the current ARDS definition, criteria for diagnosis, epidemiology, and the pathophysiology of disease. This thesis will focus on the alveolar epithelium in lung injury, which may result in ventilator-induced lung injury (VILI) and ultimately ARDS-associated lung fibrosis. It will provide an overview of the three major cellular sources contributing to pulmonary fibrosis and focus on one major mechanism called the epithelial-mesenchymal transition (EMT), where epithelial cells undergo a number of processes to transform into a fibroblast-like mesenchymal phenotype. The thesis will narrow into specific novel molecules, such as Midkine (MK) and Notch2, which have been shown to regulate EMT signaling via the angiotensin converting enzyme (ACE), a major component of the renin-angiotensin system in human lung epithelial cells. This thesis will specifically focus on the novel role of Caveolin1 (Cav1).

The work demonstrated in this thesis supports an essential role of the transmembrane molecule Cav1 in the MK-Notch2-ACE signaling pathway of ARDS-associated pulmonary fibrosis. Our findings demonstrate that Cav1 plays an important role in ACE and EMT expression in human lung epithelial cells, and suggests its potential for translation as a therapeutic target for ARDS-associated pulmonary fibrosis.

1-1 PULMONARY PHYSIOLOGY

The average human takes 20 breaths per minute, which is equivalent to 672, 768, 000 breaths in a lifetime in a person who lives up to 80 years of age. Needless to say, the lungs serve a crucial function in the organ system in order to support life. The primary function of the lung is to conduct gas exchange, but the lungs also serve to filter and act as a reservoir for blood. Within the respiratory system, deoxygenated blood enters from the right ventricle of the heart to the lungs via the pulmonary arteries. The pulmonary arteries branch into the tiny capillaries which eventually reach the alveolar space- and it is at this site where gas exchange occurs.

Oxygen enters the human respiratory system through inspired air which is conveyed by two zones- the conducting zone and the respiratory zone. The conducting zone consists of the nose, pharynx, larynx, trachea, bronchi, bronchioles, and terminal bronchioles. The conducting zone functions to filter, warm, and moisten the air, and acts as a continuous passageway for oxygen to enter and carbon dioxide to exit the lungs.

The airway epithelium, which makes up the structural component of the conducting zone, functions as an interdependent unit to act as the central defense against pathogens and inhaled

particulates from the environment [4]. The trachea epithelium consists of ciliated pseudostratified columnar cells, Goblet cells, and Clara cells, and is reinforced by C-shaped rings of cartilage which prevent it from collapsing during greatly increased pressure. Goblet cells produce and secrete mucus onto the epithelial lining, and the cilia of the columnar cells function to sweep mucus and other foreign components upwards and into the gastrointestinal tract. Clara cells are believed to secrete another substance contributing towards maintenance of the mucus lining. As we move further down the respiratory tract, the large bronchi and bronchioles possess more mucus glands and the C-shaped cartilage rings transition into fragmented hyaline cartilage plates. The terminal bronchioles move from a ciliated columnar to a cuboidal epithelial layer, exhibit less Goblet cells, and are absent of cartilaginous tissue [5, 6]. The terminal bronchioles lead into the respiratory zone of the lung.

The respiratory zone, which consists of the respiratory bronchioles, alveolar ducts, and alveoli, is the site of respiration where oxygen and carbon dioxide exchange with the blood. The respiratory bronchioles, where 10% of gas exchange occurs, varies from simple ciliated columnar epithelial cells to cuboidal epithelial cells to squamous epithelial cell types, and possesses thick segments of smooth muscle cells underneath the epithelium. Alveolar ducts communicate with alveolar sacs which divide into numerous alveoli, and this is the site where 90% of gas exchange occurs.

The alveolar epithelium consists mainly of alveolar Type I and Type II cells. Alveolar Type I cells are simple squamous cells which make up approximately 93% of the epithelial surface and is the major cell type involved in gas exchange between the alveoli and the blood [7]. Alveolar Type I cells are extremely thin and spread out widely across the surface, typically possess low

metabolic activity, and are found in close association with pulmonary capillaries. The special characteristics of alveolar Type I cells allows for increased surface area and efficient permeability of gases. There are 500 million alveoli within the human lung, which as a result gives rise to an incredibly large surface area of approximately 50 to 100 square meters for gas exchange. The basement membrane of the alveolar Type I cells fuse with the basement membrane of the pulmonary endothelial cells to form the blood-gas barrier. The blood-gas barrier is the specific site of the respiratory zone where gas exchange occurs.

Alveolar Type II cells are simple cuboidal epithelial cells found within the alveolar epithelium and comprise only a small fraction of the epithelial population, making up only 7% of the alveolar surface [7]. There are holes on the glycocalyx at the apical end of the alveolar Type II cell through which precursors of surfactant proteins are secreted. The precursors of surfactant molecules are actively converted to its final surfactant product, and surfactants are distributed by the ring of microvilli present on the epithelial surface. Pulmonary surfactants reduce surface tension caused by constant distension and recoil of the alveoli, and serve to maintain a healthy, intact epithelium. Unlike the alveolar Type I cell, the globular-shaped Type II cells are highly metabolic in function. Alveolar Type II cells are also known as progenitor cells, or defenders, which may proliferate and give rise to both Type I and Type II cells [8].

Alveolar macrophages are another cell type typically found roaming within the alveolar space. Unlike the ciliated columnar cells of the respiratory tract, alveolar Type I and Type II cells do not possess cilia, and thus, are unable to form a mucociliary escalator to remove debris or foreign particles. Therefore, the lung macrophages primarily reside in the alveoli and serve to

phagocytose residual surfactants, foreign material, and maintain the integrity of the alveolar surface.

The interstitium, otherwise known as the extracellular matrix layer located between the blood-gas barrier, is primarily constituted of Type IV collagen which is responsible for the strength of the wall. Resident lung fibroblasts are the major cell type found within the connective tissue layer of the interstitium. Lung fibroblasts primarily function to secrete extracellular matrix components and maintain the elasticity and strength of the connective tissues. Despite the strength and elasticity of the extracellular matrix, however, the blood-gas barrier is extremely thin and fragile. Therefore, the blood-gas barrier may be susceptible to alveolar leakage upon ultrastructural changes either due to increased pressure, direct injury to epithelial cells, or injury of the endothelium through indirect mechanisms.

Considering the crucial functions of the respiratory system, the lungs can no longer serve its purpose if the alveolar epithelium is exposed to injurious agents. In ARDS patients, substantial injury to the lungs, either directly to the alveolar epithelial cells or indirectly through the pulmonary circulation, render the alveolar sacs useless. Pulmonary fibrosis is often found in patients with ARDS, and mechanical ventilation is the major supportive therapy for ARDS. However, prolonged ventilation may aggravate and worsen pulmonary fibrosis and lead to high mortality. Therefore, novel therapeutic strategies are required to target and treat ARDS-associated fibrosis.

1-2 ARDS

1.2.1 ARDS Definition

ARDS, is a severe clinical condition characterized by an acute onset of increased lung permeability and pulmonary edema associated with severe arterial hypoxemia [1]. ARDS was first described in 1967 by Thomas Petty, David Ashbaugh, D. Boyd Bigelow, and Bernard Levine when 12 patients exhibited an acute onset of tachypnea, hypoxemia, and loss of compliance with no response to therapy during World War I [9]. The clinical manifestation of this condition was similar to an existing pulmonary disease called infantile respiratory distress syndrome. Infantile respiratory distress syndrome was known to result in ventilator failure caused by developmental insufficiency of surfactant production in premature infants. Thus, Petty *et al*. coined the term "adult respiratory distress syndrome" in adults.

In 1994, the American-European Consensus Conference (AECC) renamed "adult respiratory distress syndrome" to "acute respiratory distress syndrome" in recognition of its manifestation in both adults and children [10]. The AECC also defined the criteria for diagnosis of ARDS as a condition having an acute onset, bilateral infiltrates of the frontal chest on radiography, a PaO_2/FiO_2 ratio of $\leq$ 200 mm Hg, and exclusion of congestive heart failure patients with pulmonary capillary wedge pressures of < 18 mm Hg.

In 2012, the ARDS Task Force announced a new definition and severity classification system for ARDS that aimed to simplify the diagnosis and better prognosticate outcomes. According to the new definition, ARDS is exhibited by an acute onset within 7 days from a predisposing clinical

insult, bilateral opacities on radiograph, and without excluding patients with cardiac failure or fluid overload. ARDS was also categorized into three cohorts based on patient PaO_2/FiO_2 ratio- Mild: 201-300 mm Hg; Moderate: 101-200 mm Hg; and Severe: < 100 mm Hg.

1.2.2 Epidemiology

1.2.2.1 Causes

ARDS is caused by any major injury to the lung, either directly with the injurious agent reaching the lung via the airways or by trauma to the chest, or indirectly with the injurious agent arriving at the lungs through the bloodstream. Indirect lung injury is usually associated with severe trauma or severe infections such as sepsis or bacterial/viral/fungal pneumonia, which are common predisposing factors for ARDS [11, 12]. However, direct lung injury, such as gastric acid aspiration or inhalation of toxic gases, are less common. The occurrence of ARDS also varies widely by geographic region, for example, malaria is the most frequent cause of ARDS in some parts of the world, but does not exist in most of North America [13].

1.2.2.2 Incidence and Mortality

Cross-sectional studies have shown that patients with ARDS represent approximately 5% of total hospitalized and mechanically ventilated patients [14]. Despite this seemingly low number, ARDS should not be seen as a rare disease with little impact on society, as it poses a massive financial burden on the public health system with patients spending an estimated 6,368,000 days/year in hospitals [15]. The incidence of ARDS in the United States is continually rising, as shown recently by the King County Lung Injury Project, reporting numbers as high as 58.7

ARDS patients per 100,000 inhabitants/year [15]. Additionally, compared to deaths associated with other widespread diseases such as breast cancer (41,528 deaths per year), AIDS (14,802 deaths per year), and asthma (4,657 deaths per year), ARDS patient mortality remains as high as 59,000 per year [16].

1.2.2.3 Long-Term Effects

Despite the challenges of overcoming ARDS in the intensive care unit, there are still a number of survivors. Recent studies have begun to investigate the long-term outcomes of ARDS patients by measuring their health-related quality of life. Most studies reported a significantly lower health-related quality of life, with major long-term consequences related to neuromuscular, cognitive, and psychological dysfunction as opposed to pulmonary dysfunction [17, 18]. Thus, ARDS is not only a daunting condition to conquer in the intensive care unit, but also affects daily life outside of the hospital.

1.2.3 Pathophysiology

1.2.3.1 Alveolar Epithelium in Lung Injury

Traditionally, the respiratory epithelium was believed to serve function as a static physical barrier; however, ongoing research has increasingly supported an active role of alveolar epithelial cells in response to physical changes and injury. Alveolar epithelial cells, which are composed of Type I and Type II cell populations, are the major structural components of the alveolar sac. Emerging evidence has shown the critical importance of the alveolar epithelium in

the development and recovery of lung injury [19, 20]. The degree of alveolar epithelial injury has also been implicated as an important predictor of outcome in ARDS patients [21, 22].

Alveolar Type I cells, which serve the primary function of respiration, are thin and are widely spread out, allowing efficient gas exchange over large surface areas. However, Type I cells are generally incapable of proliferation and thus cannot undergo cell cycle processes to reproduce its population during circumstances such as injury. Upon exposure to pathogens, Type I cells release inflammatory mediators, undergo apoptosis, or lose polarity and structure in a process known as epithelial-mesenchymal transition (EMT).

However, Alveolar Type II cells have been shown to possess proliferative functions under development and injury. Type II cells act as a progenitor population to generate more Type I and Type II cells, but due to their small population the entire alveolar epithelium cannot be recovered during lung injury. Furthermore, Type I cells are induced to undergo EMT, gaining a migratory phenotype and actively contribute to the pathogenesis of the lung.

1.2.3.2 VILI

Mechanical ventilation (MV) currently serves as one of the major supportive therapies for ARDS patients. MV allows the respiratory muscles to rest while providing adequate gas exchange to the injured lung [23]. Patients with moderate or severe ARDS depend on MV for life support, and are thus reported to have zero ventilator-free days from the beginning of diagnosis [1]. Traditionally, patients are mechanically ventilated at high tidal volumes of 10 to 15 ml per kilogram of body weight, compared to the normal range of 7 to 8 ml per kilogram [24]. High ventilation is usually required because lung volumes are severely reduced, due to partial collapse

of the lung or leakage of edema which prevents aeration by the lung epithelium [25, 26]. However, high airway pressures may aggravate the lung by excessive distension. A multicenter randomized study conducted by The Acute Respiratory Distress Syndrome Network compared ARDS patients with high volume (12 ml per kilogram of body weight) and low volume (6 ml per kilogram of body weight) MV [27]. Strikingly, the study demonstrated that mortality was significantly lower in the group treated with low volume than the group treated with high volume MV. Thus, high volume MV may contribute to worsening of the lung, whereas low volume MV seems to have a protective effect on the lung.

VILI is characterized by physiological and morphological alterations of the lung caused by MV, resulting in structural and biochemical consequences in the airways of ARDS patients. The forces generated by MV may lead to VILI through structural and biochemical consequences within the alveolar space. Injurious MV may result in "volutrauma," physical changes in the lung due to overdistension of the alveoli, and "biotrauma," the aberrant activation of cellular signaling pathways which may result in an inappropriate fibrotic response to lung injury [28]. Oxygen delivery to ARDS patients can lead to "volutrauma", or lung stretching by MV, which leads to increased permeability of the alveolar-capillary barrier. These morphological changes result in accumulation of pulmonary edema in the lungs of ARDS patients, diffuse alveolar damage, and additional leakage due to MV.

Another major mechanism of VILI is not only by the structural disruption of the epithelium via MV, but is in fact due to "biotrauma", or biologic alterations of the lung. Activated epithelial cells, immune cells, and fibroblasts secrete inflammatory mediators such as Tumor necrosis

factor-α (TNF-α), β-catenin, Interleukin-8 (IL-8), Interleukin-6 (IL-6), and Interleukin-1β (IL-1β) [23]. Furthermore, fibrotic factors such as hydroxyproline and Transforming growth factor-β (TGF- β) may also promote hyaline membrane formation along the alveolar wall as a result of extracellular matrix secretion from activated fibroblasts [29]. Angiotensin II, a major hormone of the renin-angiotensin system, is also known to participate in fibrosis through stimulating TGF- β production [30].

1-3 ARDS-ASSOCIATED FIBROSIS

1.3.1 VILI-Associated Fibrosis

MV has been shown to aggravate the lung during the reparative process, resulting in a process known as VILI, which may contribute further to the development of fibrosis in ARDS patients [2, 3, 31, 32]. In ARDS patients, the repair process of the lung typically involves two distinct phases- a reparative phase and a fibrotic phase. The reparative phase is defined by a process where injured cells are replaced and replenished by the same cell type. The fibrotic phase is the process by which newly synthesized connective tissues replace the normal parenchyma tissue. In patients with VILI-associated fibrosis, the tissue repair process of the lung becomes pathogenic when it is not controlled. Improper regulation of the fibrotic process results pulmonary fibrosis, in which the synthesis and deposition of new extracellular matrix components exceeds the rate at which it is degraded.

Mortality remains excruciatingly high in patients- particularly in those with moderate (32%) and severe (45%) ARDS [1]. ARDS patients with longer duration of MV exhibit greater fibrosis than

those who were ventilated for a shorter period of time [33]. In fact, autopsy studies have identified pulmonary fibrosis as a common feature patients with ARDS [34]. A prospective study of open-lung biopsies conducted over the course of an 8-year period found that 53% of ARDS patients exhibited fibrosis with MV [35]. Furthermore, a study demonstrated that 64% of mechanically ventilated patients developed pulmonary fibrosis leading to a subsequent mortality rate of 57%, compared to zero mortality in patients with no fibrosis [31]. In addition, clinical studies have demonstrated that mechanically ventilated patients with late ARDS exhibit ongoing inflammation and progressive fibrosis as shown by lung histology [36, 37]. Moreover, ARDS patients 7 days after diagnosis were presented with significantly elevated levels of transforming growth factor-α and procollagen peptide III, both of which are potent biological markers of fibroproliferation [29].

These data support our findings that pulmonary fibrosis is exhibited by many ARDS patients. Resolving fibrosis early on may be the key factor to reduce mortality rates in ARDS (**Figure 1**). The following sections will focus on the major mechanisms of pulmonary fibrosis and expand deeply into one major source which will be the focus of this thesis.

1.3.2 Mechanisms of Fibrosis

Previously, it was believed that local tissue myofibroblasts were the primary source of fibrosis, through the excessive production of extracellular matrix components following initial injury [38]. However, recent studies challenged this view of fibrosis with the hypothesis that fibrosis may be attributed by other cellular sources in addition to resident fibroblasts [39-41]. The change in

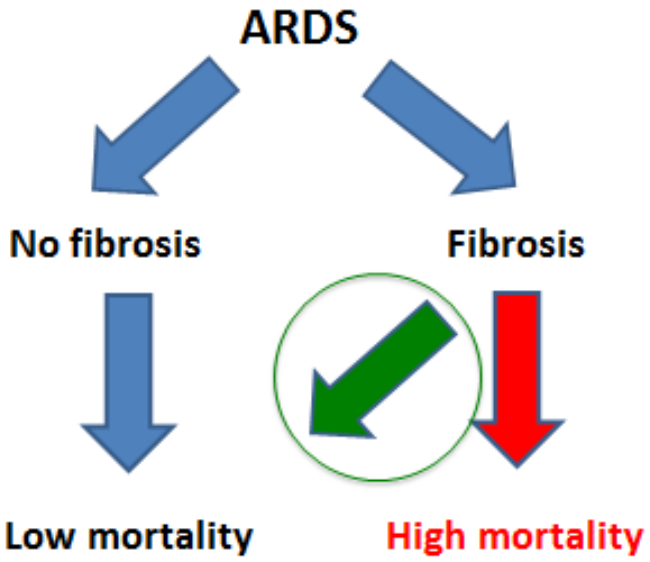

Figure 1. Resolving lung fibrosis may reduce mortality rates in ARDS patients. ARDS patients with no pulmonary fibrosis have low mortality rates. However, patients with evidence of fibrosis have high mortality rates. Resolving lung fibrosis early on may be the key factor to reduce mortality in ARDS. This was previously overlooked but is now a central focus of ARDS pathophysiology.

paradigm has significantly altered the widely accepted traditional view of fibrosis and brought about novel mechanisms responsible for fibrotic development.

Many studies, particularly in the context of renal fibrosis, have supported the critical role of resident fibroblasts but have also hypothesized that alternative cellular sources of fibrosis may exist [42-44]. In the kidney, a diverse origin of fibroblasts has been proposed which may lead to activation and formation of myofibroblasts. One of the most well-established and widely accepted sources is due to interstitial resident fibroblast activation and proliferation of the renal tissue. Another source of myofibroblasts may originate from pericytes, which are contractile cells that wrap around the endothelial cells of capillaries and venules. Activated pericytes may differentiate upon stimulation and contribute towards deposition of extracellular matrix components. In addition, fibrocytes, immature fibroblasts that circulate within the peripheral blood, may also be recruited to the site of fibrosis through profibrotic cytokine release of resident fibroblasts. Fibrocytes may settle in the connective tissues and actively contribute towards collagen production during fibrosis. A critical source of renal fibrosis has also been shown to be contributed by activation of epithelial cells which undergo a process called EMT to acquire phenotypic characteristics of a myofibroblast. Additionally, renal endothelial cells may become activated and undergo a similar process to that of tubular epithelial cells, called endothelial-mesenchymal transition (EndoMT).

Thus, there are a number of cellular sources which may contribute towards myofibroblast activation in the context of renal fibrosis. Interestingly, it has been demonstrated by numerous studies that renal fibrosis and pulmonary fibrosis share a number of similar characteristics in

regards to phases of resolution and activation of specific molecular signaling pathways upon injury. Therefore, it is not surprising that renal and pulmonary tissues may share similar underlying cellular sources contributing to fibrosis.

The pathophysiology of VILI-associated pulmonary fibrosis has been proposed to be attributed to a number of cellular sources and mechanisms. Pulmonary fibrosis is comprised of three major processes: 1) Expansion of the resident lung fibroblast population, 2) increased recruitment of circulating fibrocytes into the lung, and 3) EMT of alveolar epithelial cells [3] (**Figure 2**).

Resident fibroblasts are mature interstitial fibroblasts that function to secrete extracellular matrix components and maintain the pulmonary connective tissues. A widely recognized cellular source of pulmonary fibrosis is due to the development of resident lung fibroblasts to a fibrogenic population of activated myofibroblasts [45]. Their transition into a myofibroblast phenotype is largely attributed to TGF-β signaling in resident fibroblasts and release of other profibrotic cytokines. Inhibition of TGF-β signaling in activated fibroblasts has shown to prevent collagen synthesis in the context of fibrotic diseases [46]. In addition, release of profibrotic mediators by activated resident fibroblasts further enhance the development of pulmonary fibrosis by recruitment of circulating fibrocytes into the lung tissue.

Fibrocytes are monocyte-derived cells with features of both macrophages and fibroblasts, and are often termed “immature fibroblasts” [47]. Fibrocytes are found circulating in the peripheral blood and have been shown to possess the ability to migrate to the lung as a progenitor of resident fibroblasts, differentiate into myofibroblasts, and constitutively produce extracellular

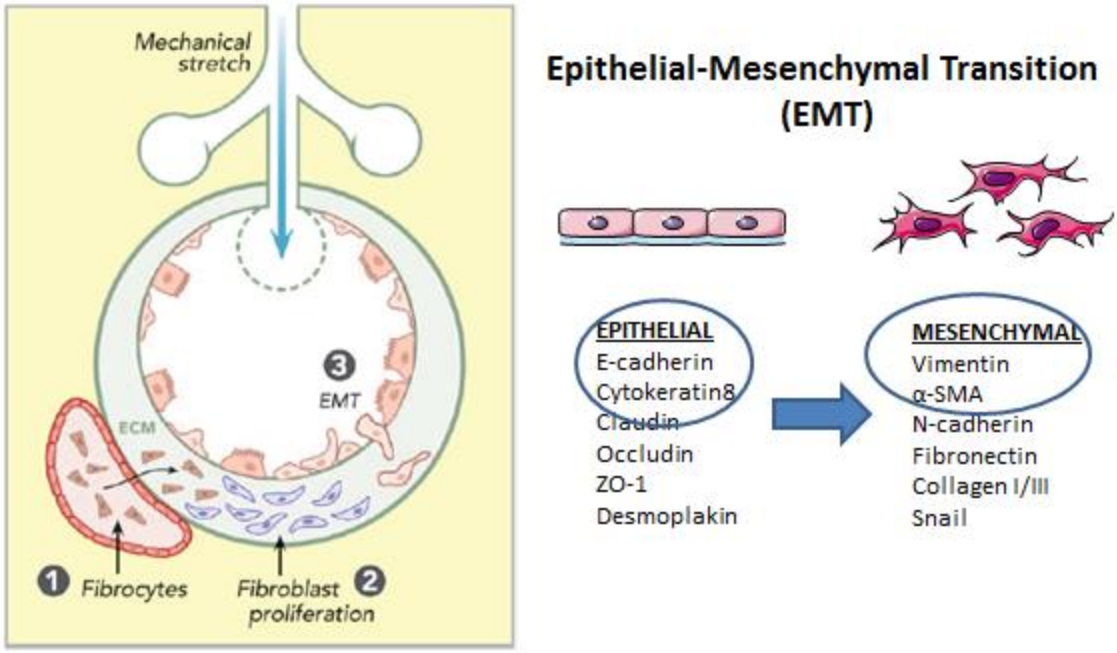

Figure 2. Three major sources of pulmonary fibrosis (left panel adapted from Cabrera-Benitez *et al.* 2014). There are three major cell sources of pulmonary fibrosis: 1. Recruitment of circulating fibrocytes into the lung, 2. Proliferation of resident lung fibroblasts, and 3. Epithelial-mesenchymal transition (EMT) of alveolar epithelial cells. EMT is a process where cells lose their epithelial characteristics and transform into a mesenchymal fibroblast-like phenotype. This can be observed through the downregulation of epithelial markers such as E-cadherin and Cytokeratin8, and the upregulation of mesenchymal markers such as Vimentin and α-SMA.

matrix components [48-51]. Alveolar fibrocytes have been found in bronchoalveolar lavage of mechanically ventilated ARDS patients, and have been established as an independent predictor of poor outcome of patients with ARDS [52]. Thus, increased recruitment of fibrocytes into the lung may be a significant contributor to VILI-associated pulmonary fibrosis.

Fibroblasts and myofibroblasts are also believed to arise not only from resident lung fibroblasts and circulating fibrocytes, but also from alveolar epithelial cells in the lung. At the site of lung injury, a host of inflammatory cytokines and profibrotic factors are released by fibroblasts and immune cells of the lung. This induces the activation of resting alveolar epithelial cells to lose their apical-basal polarity and undergo a change to a mesenchymal phenotype. The intermediate stage of this process is termed “epithelial-mesenchymal transition” or EMT. Epithelial cells that lose their polarity undergo major cytoskeletal changes, with a loss of adherence to surrounding epithelial cells and the basement membrane layer, and become motile in order to invade into the underlying connective tissue layer. Upon migration to the interstitium, lung epithelial cells assume characteristics similar to myofibroblasts by secretion of extracellular matrix components into the fibrotic environment and enhancing the development of pulmonary fibrosis. The following section will focus more in depth in the mechanism of EMT and its relevance *in vitro* to investigate VILI-associated pulmonary fibrosis.

1.3.3 Epithelial-Mesenchymal Transition

EMT is a process that is characterized by morphological changes of a cell from an adhesive, polarized state with an organized cytoskeletal structure towards a loss of polarization, enhanced pseudopodia formation, and ultimately a gain of an invasive phenotype. EMT may be defined by

a loss of lung epithelial markers which includes proteins present in the adherens junctions and cytoskeletal components in order to maintain the attachment of epithelial cells to each other and maintain their polarity. Common epithelial markers which are widely used in the literature to study EMT are E-cadherin and Cytokeratin8. EMT can also be visualized by the gain of expression of lung mesenchymal markers, such as α-SMA and Vimentin [32, 53].

EMT is a major critical process during development for tissue development. During embryogenesis, cell migration and differentiation is tightly regulated through interplay of extracellular and intracellular signaling via EMT. Cells move back and forth from epithelial and mesenchymal states to form the epithelial lining and supporting tissues [53]. During gastrulation, cells communicate with each other through cell-cell contact in order to form a three-layered structure known as the gastrula. The gastrula is made of three major layers called the ectoderm, mesoderm, and the endoderm, and eventually develops into functional organs and tissue components of the human body. The respiratory tract of the lungs arises from the innermost endoderm layer.

EMT is also detected upon aberrant activation of cell signaling during tissue repair processes in adults. EMT has been shown to play a critical role in major diseases, and may be visualized primarily in the context of tumor metastasis and organ fibrosis. Lung EMT of alveolar epithelial cells is a major proposed source of ARDS-associated pulmonary fibrosis. Evidence of lung EMT *in vivo* supports the role of contributing to fibrotic development in pulmonary fibrosis [54]. It has also been demonstrated that MV further enhances the profibrotic phase through EMT in vivo studies of ARDS [32]. Interestingly, EMT has been shown to be activated by the renin-

angiotensin system specifically through the ACE-mediated production of the profibrotic molecule Angiotensin II. Therefore, ACE and its product Angiotensin II may play a major role in in renal and pulmonary fibrosis [55-58]. However, the specific molecular mechanisms leading to EMT remain to be elucidated.

EMT is a major cellular source of VILI-associated pulmonary fibrosis, yet its mechanism of activation is unknown. Fibrosis is associated with high mortality rates in patients with ARDS, and furthermore, MV, the major supportive therapy for ARDS, has been shown to contribute to VILI. The concept of EMT offers an advantage in that it may be studied *in vitro* though examination of the characteristics of lung epithelial cells undergoing EMT to a mesenchymal phenotype in the cell culture setting. Therefore, investigating novel targets involved in EMT signaling at the molecular level may shed light on novel therapeutic strategies for ARDS-associated pulmonary fibrosis.

1.3.4 Novel Mediators Contributing to ARDS-Associated Fibrosis

1.3.4.1 Midkine

Midkine (MK) is a 13 kDa cytokine and heparin-binding growth factor that has been shown to regulate proliferation, differentiation, migration, apoptosis, and other critical cellular processes [59]. During the midgestation stage of embryogenesis, MK is strongly upregulated in order to stimulate mesenchymal tissue development, however, its expression is generally very low in normal adult tissue [60]. Interestingly, MK expression has been shown to be potently activated upon injury, during processes such as acute and chronic inflammation [61] and tissue repair [59].

MK has recently been established as a novel regulator of chronic kidney disease and renal fibrosis via its regulation of Angiotensin I-converting enzyme (ACE), a crucial component of the renin-angiotensin system [62, 63]. Additionally, studies have shown a role of MK in modulating EMT in pancreatic ductal adenocarcinoma cells [64] and immortalized HaCaT keratinocytes [65]. Further investigations have subsequently demonstrated a novel role for MK in the lung epithelium and endothelium in ACE activation and EMT [66, 67].

Although receptors for MK have not yet been fully elucidated, current literature has shown that MK binds to several plasma membrane receptors to activate various cellular events: LDL receptor-related protein (LRP) in cell survival [68], $\alpha_4\beta_1$- and $\alpha_6\beta_1$- integrins in cell migration [69], anaplastic lymphoma kinase (ALK) in cell proliferation [70], and receptor-type tyrosine phosphatase ζ (RPTPζ) in immune cell regulation [71]. Recently, Notch2 was discovered as the first potential MK receptor responsible for pathogenesis of cell signaling [72].

1.3.4.2 Notch2 in EMT

Notch was first discovered approximately 100 years ago, upon mutation of the Notch gene which resulted in the formation of notches at the wing margin in *Drosophila* [73] The human Notch family is comprised of four proteins- Notch1, Notch2, Notch3, and Notch4- which are transmembrane receptors possessing highly conserved protein structure and expression in human tissues [74, 75] (**Figure 3**). Each protein contains a stretch of 29-36 tandem epidermal growth factor-like (EGF) repeats and 3 Lin-12/Notch repeats (LNR) in the extracellular domain (ECD), and 6 Ankyrin repeats and a PEST-containing region in the intracellular domain (ICD) [76].

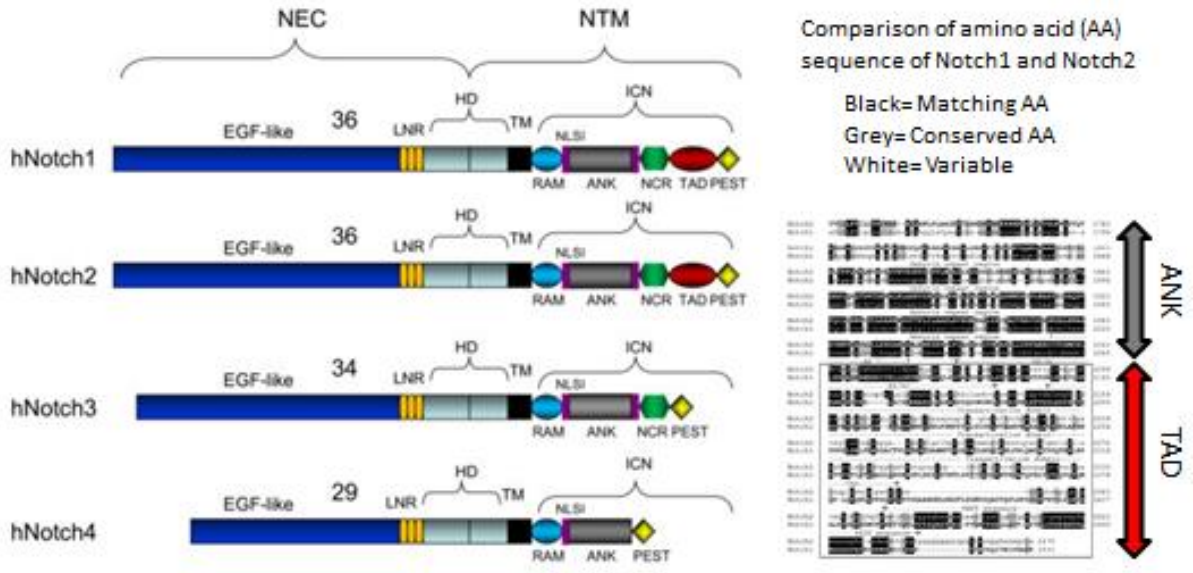

Figure 3. Notch family receptor structures are highly conserved except at the transactivation domain (TAD) in the intracellular domain (left panel adapted from Pancewicz *et al*. 2011; right panel adapted from Kraman *et al*. 2005). The left panel shows the structure of the Notch receptors. Notch2 is part of a widely known four-member family of receptors- Notch1, Notch2, Notch3, and Notch4. Notch1 and Notch2 are highly conserved, but there is a highly variable region called the TAD in the intracellular domain. The right panel shows the difference in amino acid sequence of the TAD in Notch1 and Notch2. The TAD may be responsible for the differences in interaction of Notch1 and Notch2 with other receptor molecules, leading to activation of different downstream signaling pathways.

Interestingly, Notch1 and Notch2 are the only proteins with a transactivation domain (TAD) within the ICD [77, 78]. The TAD is a specific amino acid sequence region located between the nuclear localization signal sequence and a glutamine-rich region called the OPA region [79, 80]. The TAD of Notch1 has been shown to associate with coactivators such as the histone acetyltransferases PCAF and GCN5 [81], and is a necessary component of signal transduction in various cell types. The binding partners of TAD of Notch2 have not been as well characterized as Notch1, but it is highly likely that the Notch2 TAD may serve a similar function by interacting with proteins to activate its downstream signaling. Whole-genome sequencing has shown that lymphoma patients exhibit recurring mutations in the Notch2 TAD region, suggesting its importance for cellular signaling in the disease context [82]. A study demonstrated that the TAD of Notch1 and Notch2 are not highly conserved and thus makes it possible for the ICDs to interact with different proteins and activate different downstream signaling pathways [83].

Notch proteins have traditionally been established as a key regulator of cell fate determination during embryogenesis and in cell proliferation and survival in adult tissues [76, 84]. Notch expression is highly upregulated during epithelial-mesenchymal transition (EMT) of embryonic tissues [85-87], but have also recently become of interest due to their emerging role in the acquisition of EMT in numerous carcinomas [88-91].

Specifically, Notch2 has recently gained interest due to its pathogenic role in cancer and fibrosis. Upon activation, ligand-receptor interaction induces a conformational change in the full-length 256 kDa Notch receptor, exposing critical sites on the transmembrane domain for proteolytic cleavage. The juxtamembrane domain undergoes the first cleavage by ADAM10/17 (disintegrin

and metalloproteinase domain-containing protein 10 or 17), followed by a second cleavage at the transmembrane domain by the γ-secretase complex. This results in the release of the activated 110 kDa ICD [92] into the cytosol to enter the nucleus and activate gene transcription [93]. Activated Notch2 regulates EMT in mesodermal tissues, and Notch2 knockout mice have shown to be embryonic lethal, thus, suggesting its crucial role during organ development [94]. Importantly, studies have demonstrated that Notch2 is a key modulator of EMT in pancreatic ductal adenocarcinoma cells [64, 72] and HaCaT keratinocytes [65]. This suggests the essential role of Notch2 in EMT processes during development and disease.

1.3.4.3 ACE in Fibrosis

Angiotensin I-converting enzyme (ACE), also known as peptiyl-dipeptidase A, kininase II, CD143, or EC3.5.15.1, is a 195 kDa zinc metallopeptidase with a critical role in a major hormone system called the renin-angiotensin system [95]. The renin-angiotensin system was first discovered in 1898 as a regulator of the cardiovascular system via the kidney [96]. Upon changes in renal perfusion pressure, tubular salt content, and sympathetic nerve activity, the juxtaglomerular cells of the kidney release active renin into the circulation. In the blood, renin cleaves liver-borne Angiotensinogen to generate the relatively inactive peptide Angiotensin I, which is then cleaved by ACE to produce the active Angiotensin II [97]. It has been shown that 90% of ACE activity takes place in the lung, therefore, the renin-angiotensin system has critical implications in the lung [98]. During normal physiology, ACE and Angiotensin II serve essential roles in local and systemic hemodynamic regulation [55].

However, ACE and its cleavage product Angiotensin II have also been found to regulate organ fibrosis. Angiotensin II, which is actively processed by ACE upon injury, is associated with upregulation of profibrotic molecules such as TGF-β [99], phosphoinositide 3-kinase [100], and Wnt/ β-catenin [57]. Furthermore, Angiotensin II induces EMT through the reactive oxygen species/Src/Caveolin-mediated activation of the epidermal growth factor receptor (EGFR) [56].

ACE and Angiotensin II have been shown to induce the upregulation of profibrotic factors, EMT, and tissue remodeling in renal, cardiac, and pulmonary fibrosis [99-101]. A study using a bleomycin model of lung injury showed that procollagen synthesis and lung collagen deposition were stimulated by Angiotensin II [99]. Administration of an ACE inhibitor called Ramipril not only significantly reduced Angiotensin II levels, but also decreased TGF-β expression and collagen deposition in rat lungs. Another study found a dramatic increase in lung lymph ACE concentration following infusion of Pseudomonas bacteremia in adult sheep [102]. Elevated levels of soluble ACE have also been found in the bronchoalveolar lavage of ARDS patients compared to healthy individuals [103].

1.3.4.4 MK-Notch2-ACE Signaling Pathway

Previously, our group discovered a significant upregulation of MK expression in the plasma of ARDS patients compared to healthy individuals [2]. We have also established a two-hit *in vitro* model of hydrochloric acid (HCl) and mechanical stretch in human lung epithelial cells, which showed an upregulation of MK with exposure to HCl and mechanical stretch [2]. We also found that MK upregulation is associated with activation of ACE and EMT, and knockdown of MK expression via transfection of MK siRNA inhibited downstream activation [2].

As previously mentioned, other studies have demonstrated that the transmembrane protein, Notch2, may serve as a potential cell surface receptor for MK in various cell types. We confirmed the protein complex of MK and the full-length Notch2 protein in human lung epithelial cells through co-immunoprecipitation assays. Furthermore, transfection of Notch2 siRNA to knock down Notch2 expression followed by subjecting lung epithelial cells to mechanical stretch blocked the ACE signaling and induction of EMT. However, it is unknown how Notch2 activates ACE expression, since there is lack of interaction between these molecules. The following chapter will focus on a novel molecule called Caveolin1, which may play a key role in mediating activated Notch2 and downstream ACE and EMT signaling.

1-4 CAVEOLIN1

1.4.1 The Caveolin Family

The Caveolin (Cav) family is comprised of three structurally similar 20-22 kDa proteins- Caveolin1 (Cav1), Cav2, and Cav3- which join together to form caveolae [104]. Caveolae, or “little caves”, are 50-100 nm omega-shaped vesicular invaginations of the plasma membrane which play a critical role in regulating endocytosis, intracellular cholesterol transport, and cell surface signaling [105-107]. Caveolin proteins are phosphorylated at Tyrosine-14 during cell stimulation such as mechanical stretch. Caveolin proteins are also known to be phosphorylated at Serine-80 near a region called the caveolin scaffolding domain (CSD), which serves to recruit and promote signaling of transmembrane receptors upon activation [108]. The CSD is a hydrophobic domain containing the Cav1 binding motif, and is located in the inner leaflet of the plasma membrane [109].

Cav1 is a transmembrane protein highly expressed in the plasma membrane of endothelial cells, epithelial cells, adipocytes, fibroblasts, and smooth muscle cells. Cav1 is required for the formation of caveolae, and thus serves as the main structural component of caveolae [110] (**Figure 4**). Cav1 has been demonstrated to regulate the interaction and subcellular distribution of crucial transmembrane receptors in cell proliferation, differentiation, adhesion, and migration.

Cav2 is a transmembrane protein which possesses similar structure as its relative Cav1, and also comprises the major component of caveolae. Cav2 is also ubiquitously expressed and is often found tightly interacting with and forming complexes with Cav1. Interestingly, studies have found that the interaction of Cav2 with Cav1 is necessary for transport of Cav2 to the plasma membrane [111, 112]. Furthermore, in the absence of Cav1, Cav2 is degraded and its expression is strikingly reduced [113]. Co-expression of Cav2 with Cav1 suggests a functional role that may be similar to that of Cav1, however, its specific role is poorly defined.

Cav3 is similar in structure and function to its family members, Cav1 and Cav2. However, Cav3 expression is specific to muscle tissues, therefore it is mainly abundant in skeletal, smooth, and cardiac muscles [114]. Cav3 plays a critical role in transduction of cell signaling in muscle cells, supported by studies showing amino acid substitutions in Cav3 are associated with patients with muscular dystrophy [115].

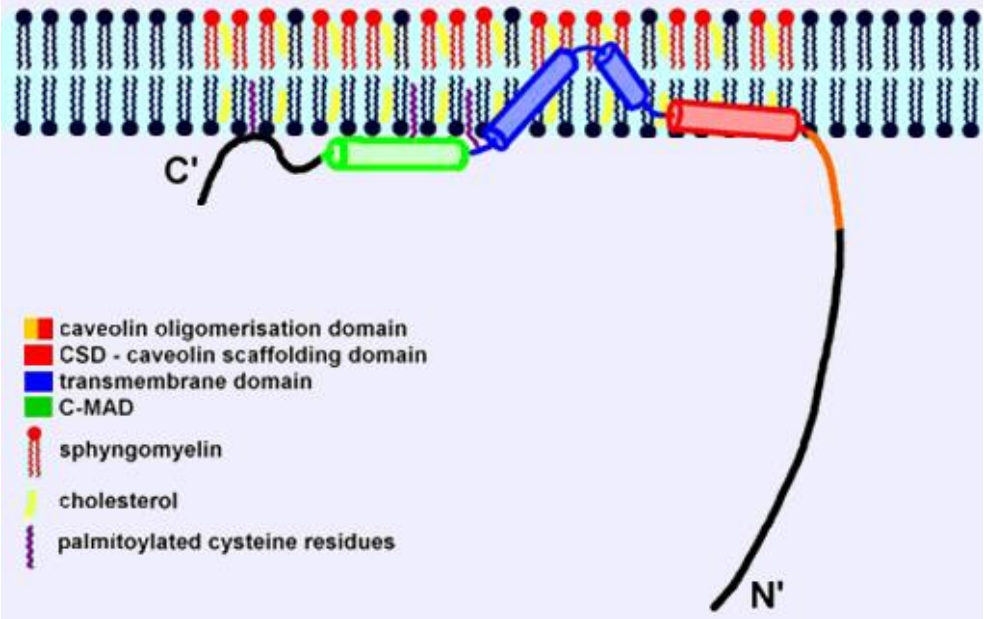

Figure 4. Structure of Caveolin1 transmembrane protein (adapted from http://atlasgeneticsoncology.org//Genes/CAV1ID932ch7q31.html). Caveolin1 (Cav1) is part of a three-member family of 20-22 kDa transmembrane proteins- Cav1, Cav2, and Cav3. Cav3 is restricted to muscle tissues, Cav2 is stabilized by the co-expression of Cav1, and thus, Cav1 is our major focus. Cav1 has a C-terminal membrane attachment domain (C-MAD), the transmembrane domain, and the caveolin scaffolding domain (CSD). Cav1 forms the main structural component of Caveolae, which form 50-100 nm omega-shaped invaginations of the plasma membrane. Cav1 regulates a number of critical cellular processes at the cell surface.

Despite the crucial functions of the Caveolin family in regulating cellular processes, Cav1 remains the major isoform which is widely investigated. Cav2 and Cav3 isoforms are not often studied due to several reasons. In lung epithelial cells, Cav2 serves a supportive or redundant function to Cav1 and requires Cav1 expression in order to carry out its purpose. Additionally, Cav3 is the major isoform found in muscle cells, and is thus not the major component of lung epithelial cells. Therefore, the focus of this study is centralized on the function and expression of the major isoform, Cav1.

1.4.2 Caveolin1 in Lung Injury

Cav1 regulates critical cellular processes such as proliferation, differentiation, endocytosis, adhesion, migration, and subcellular distribution of transmembrane proteins at the plasma membrane to activate downstream signaling, and has also been implicated to play a role in inflammation and fibrosis [116, 117]. Cav1 has been demonstrated to concentrate a wide variety of signaling molecules at the plasma membrane, including glycosyl phosphatidylinositol-linked proteins, Src-family tyrosine kinases, H-Ras, heterotrimeric G protein subunits, protein kinase C isoforms, and endothelial nitric oxide synthase [106, 110]. Cav1 is highly abundant in the majority of cell types in the lung, including epithelial, endothelial, connective tissue cells, and alveolar macrophages [118].

The role of Cav1 has been previously investigated in various models of lung injury using Cav1 knockout mice. In a study by Maniatis *et al.*, Cav1 knockout mice and wild type mice were ventilated for up to 6 hours using protective (8 ml/kg body weight) and injurious (21 ml/kg) MV to demonstrate that Cav1 knockout mice are more resistant to VILI [119]. Cav1 knockout mice

exhibited a significant decrease in lung permeability as measured by albumin accumulation, and showed a reduction in inflammation via cytokine levels in bronchoalveolar lavage and numbers of recruited neutrophils to the lung. Upon rescue of Cav1 expression, alveolar epithelial response to injury is restored in mice. In another study, Shivshankar *et al.* induced pulmonary fibrosis in mice using intratracheal instillation of bleomycin in Cav1 knockout mice and wild type mice [120]. Cav1 knockout mice were more found to be more resistant to bleomycin-induced pulmonary fibrosis compared to wild type mice. Cav1 knockout mice exhibited significantly less collagen deposition as defined by significantly reduced procollagen mRNA and α-SMA expression. Taken together, these results support the role of Cav1 in promoting lung injury.

Other studies using models of VILI suggest that Cav1 may serve a protective function in the lung. A study by Le Saux *et al.* subjected Cav1 knockout mice and wild type mice to 7.5 ml/kg MV and demonstrated that Cav1 knockout mice actually exhibit more severe lung injury and increased collagen deposition compared to wild type mice [121]. Another study by Hoetzel *et al.* found that MV at 12 ml/kg for 8 hours resulted in a more severe lung injury in Cav1 knockout mice compared to wild type mice [122]. These studies seem to suggest that Cav1 may serve to mediate protective effects upon lung injury.

It seems that Cav1 plays a context-dependent role, and differences in findings may be attributed to various conditions and models of pulmonary fibrosis. It is worthy to note that Cav1 knockout mice do exhibit hypercellularity in the alveolar space. Cav1 knockout mice possess a thickened alveolar wall which results in constricted and irregular alveolar spaces [109]. However, a critical point must be raised in regards to the hypercellular phenotype of Cav1 knockout mice- studies

have demonstrated that only the pulmonary endothelium exhibits this feature, whereas the alveolar epithelium remains unaffected [113, 123]. Therefore, it may appear that Cav1 knockout mice may possess increased susceptibility to VILI.

Interestingly, this is not the case in many studies of Cav1 and lung injury, suggesting that the role of Cav1 may depend on the context, stage, and condition of experimental diseases. For example, Cav1 knockout mice show a significant reduction in collagen deposition and synthesis in a model of idiopathic pulmonary fibrosis [120]. In contrast, Cav1 manifests a difference in the response to various models of VILI, where varying conditions of mechanical ventilation have been used. In these cases, it may be crucial to find relevance to the clinical setting. For example, VILI would occur with injurious ventilation of 21 ml/kg for 8 hours, in comparison to a mere 12 ml/kg. As previously stated, ARDS patients are mechanically ventilated at higher volumes due to reduction in airway spaces. Cav1 may thus play an important role in regulating lung injury and ARDS-associated fibrosis. The specific mechanism of Cav1 must be investigated in order to determine its clear role in the context of pulmonary fibrosis.

1.4.3 Caveolin1 in Tumorigenesis EMT

EMT has been recognized as a central feature of the pathological transitions that occur during the progression of epithelial tumors. EMT allows cancer cells to transform into a phenotype characterized by increased motility and invasiveness, thus promoting tumor metastasis and malignancy. Numerous kinases and G-proteins such as Src-family tyrosine kinases, H-Ras, integrins, Wnt/β-catenin, and Notch mediate oncogenic pathways which induce EMT [124]. As

previously stated, Cav1 is reported to facilitate the signaling of many of these growth factors in the context of lung injury, and thus may play a major role in EMT in cancer.

Cav1 expression has been assessed in a wide range of human carcinomas and sarcomas. Interestingly, Cav1 expression is upregulated or downregulated depending on the tumor cell type, and maintains consistency within tumors derived from the same type of tissue [106]. For example, many investigations have shown that Cav1 is consistently upregulated in bladder [125, 126], esophageal [127], thyroid [128], and prostate [129] carcinomas. Other studies have demonstrated that Cav1 expression is downregulated in ovarian [130], mammary [131-133], and cervical [134] carcinomas. In the lung, Cav1 expression is aberrantly upregulated in the metastatic subpopulation and is significantly correlated with overall patient survival rate and advanced pathologic stage of the pulmonary squamous cell carcinoma [135].

There is a growing body of evidence supporting the role of Cav1 in promoting metastasis. In a model of prostate cancer, mouse metastasis-derived cell lines exhibited Cav1 upregulation compared to primary tumor-derived cells [136]. Furthermore, Cav1 expression is upregulated in human metastatic prostate cancer, and its antisense-mediated downregulation reduced their metastatic phenotype [137]. Increased expression of Cav1 has also been reported to promote EMT in various non-small-cell lung carcinoma lines [138]. Other studies have demonstrated that overexpression of Cav1 is correlated with metastasis in esophageal [127], renal [139], and lung [140] carcinomas/adenocarcinomas.

It is clear that Cav1 plays an important role in EMT in various cancers and models of fibrosis. Studies have yet to elucidate the specific mechanism of Cav1 in the EMT process of pulmonary fibrosis. The following sections aim to address the potential novel regulatory mechanism of Cav1 in the MK-Notch2-ACE signaling pathway of EMT in the lung.

1.4.4 ACE and Caveolin1

Previous investigations suggest that Cav1 and ACE individually are critical for the physiological and pathophysiological processes in the lung. Cav1 is a transmembrane protein required for numerous cellular processes and is ubiquitously expressed within the pulmonary tissue, and ACE is a major component of the renin-angiotensin system, which is highly active in the lung endothelium and epithelium.

Interestingly, several studies suggest the potential relationship of Cav1 in regulating ACE expression in the lung. A study by Maniatis *et al.* observed significantly reduced lung ACE expression and activity in whole lung tissues of Cav1 knockout mice compared to wildtype mice [141]. The effect of Cav1 on ACE was visible primarily in the lung but not in other major organs such as the brain, liver, and heart tissues. Another study by Uyy *et al*. demonstrated that an increase in lung Cav1 expression is associated with a significant increase in ACE expression in a mouse model of diabetes [142].

These studies seem to support a regulatory relationship of Cav1 on activating ACE expression in the lung. Furthermore, Cav1 and ACE have not been explored together in the context of EMT,

which may reveal a Cav1 as a novel target in translation of the signaling and activation of pulmonary fibrosis.

1.4.5 Notch and Caveolin1

Previously, it was thought that Cav1, which make up invaginations of the cell surface, served to deliver cholesterol and endocytose proteins at the plasma membrane. However, a novel role of Cav1 has been supported by recent studies suggesting that Cav1 may sequester and promote the activation of transmembrane proteins through their subcellular concentration. In light of this emerging role, Cav1 sequencing revealed a hydrophobic region within the protein called the CSD. The CSD has been shown to interact with many proteins with important signaling cascade functions, such as glycosyl phosphatidylinositol-linked proteins, Src-family tyrosine kinases, H-Ras, heterotrimeric G protein subunits, protein kinase C isoforms, and endothelial nitric oxide synthase. However, a direct interaction of Cav1 and Notch2 has not been established in literature.

Interestingly, several studies have speculated a relationship between Cav1 and the transmembrane receptor Notch in the context of neural differentiation. In a study by Li *et al.*, brain tissue sections of Cav1 knockout mice revealed a significant decrease in activated Notch and the downstream Notch components compared to wildtype mice [143]. Furthermore, knockdown of Cav1 expression in neural progenitor cells also resulted in a large reduction in Notch expression and its components. Overexpression of Cav1 in neural progenitor cells using a human recombinant Cav1 induced a drastic increase in activated Notch expression. In another study by Wang *et al*., Cav1 was demonstrated to modulate Notch signaling in mesenchymal

stromal cells [104]. These studies support a potential regulatory role of Cav1 on Notch, however, these molecules have not been linked directly in literature.

These studies suggest a possible mechanism of Cav1 mediating Notch and ACE signaling, subsequently leading to the EMT pathway. The study herein investigates whether Cav1 may serve as the key mediator between Notch2 and ACE in human lung epithelial cells.

Chapter 2
Rationale, Hypothesis and Objectives

2.1 Rationale

Mortality rates remain excruciatingly high (45%) in patients with severe ARDS. MV is widely used as the major support therapy, since there are no effective pharmacologic therapies available. However, prolonged MV may promote pulmonary fibrosis, resulting in a condition termed as VILI. The development of pulmonary fibrosis has been shown to be associated with high mortality in ARDS patients. Thus, novel therapeutic targets are required to modulate the fibrotic response of the lung in ARDS-associated fibrosis.

There are three major cellular sources which contribute to pulmonary fibrosis: 1) Expansion of the resident lung fibroblast population, 2) increased recruitment of circulating fibrocytes into the lung, and 3) epithelial-mesenchymal transition (EMT) of alveolar epithelial cells. EMT is a major mechanism by which epithelial cells give rise to an activated myofibroblast-like mesenchymal phenotype in the context of cancer and fibrosis. Numerous studies have demonstrated the role of the renin-angiotensin system components, ACE and Angiotensin II, in EMT as well as renal and pulmonary fibrosis. EMT is the focus because the lung epithelium is the target of injury during ARDS.

Interestingly, a novel 13 kDa cytokine called MK has been associated with EMT and has also been implicated to modulate ACE signaling in renal fibrosis. Our group demonstrated that MK expression is significantly elevated in the plasma of ARDS patients within 24 hours of diagnosis. Our group developed a two-hit *in vitro* model of HCl and mechanical stretch, where upregulation

of MK was induced and also led to increased ACE and EMT signaling in human lung epithelial cells. Studies in pancreatic ductal adenocarcinoma cells and human keratinocytes demonstrated that MK may bind to a transmembrane receptor Notch2. We confirmed the binding of MK and Notch2 in human lung epithelial cells to demonstrate that Notch2 indeed serves as the cell surface receptor for MK. Furthermore, knockdown of MK and Notch2 individually resulted in a block in downstream ACE and EMT signaling. Our results established that the MK-Notch2-ACE signaling pathway is responsible for EMT in human lung epithelial cells (**Figure 5**). However, it is important to note that the mechanism by which Notch2 leads to activation of downstream ACE and subsequent EMT signaling is largely unknown. Thus, it is crucial to find the molecule that links Notch2 and ACE to mediate EMT in human lung epithelial cells.

Cav1 is a transmembrane protein that serves as the major structural component of caveolae, which are invaginations of the plasma membrane that regulate endocytosis. Several studies revealed that Cav1 may play an important role in VILI and ARDS-associated pulmonary fibrosis. Cav1 has also been linked to EMT in various *in vitro* and *in vivo* studies, suggesting its role in a more specific context. Interestingly, Cav1 has been shown to regulate downstream ACE signaling *in vivo*. Cav1 knockout mice demonstrated a wide reduction in ACE expression and activity in whole lung tissues compared to wildtype mice. In addition, Cav1 overexpression was associated with a significant increase in ACE expression *in vivo*. Furthermore, Cav1 has been shown to modulate Notch receptor expression in several models of neural differentiation. Knockdown of Cav1 expression resulted in significantly reduced expression of activated Notch *in vivo* and *in vitro*.

These studies together suggest a potential relationship between Notch, Cav1, and ACE, supporting the central role that Cav1 may play in this signaling pathway. The study herein investigates whether Cav1 may serve as the key mediator of Notch2 and ACE in the MK-Notch2-ACE signaling pathway on EMT in human lung epithelial cells.

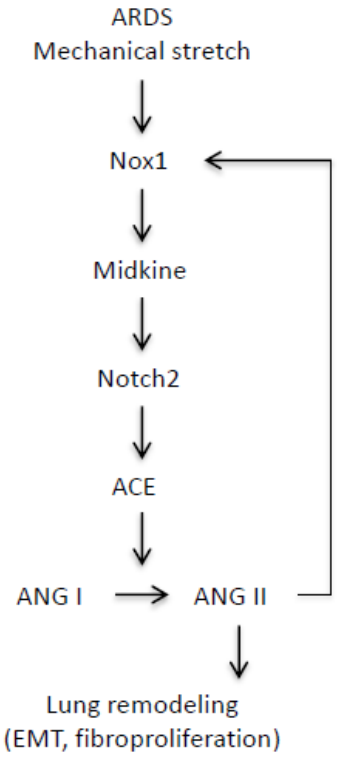

Figure 5. The Midkine-mediated signaling pathway of lung fibrosis in ARDS (adapted from Zhang *et al.* 2015). This schematic exhibits the previously established MK-Notch2-ACE signaling pathway from *in vitro* and *in vivo* experiments conducted by our group. Our data confirms MK as a novel regulator of lung remodeling via binding to cell surface receptor Notch2 to activate downstream ACE and EMT signaling in human lung epithelial cells. However, there is a lack of interaction of Notch2 and ACE. This thesis investigates the link between Notch2 and ACE, and sheds light on a molecule called Cav1, which may be the key mediator in this pathway.

2.2 Hypothesis

Caveolin1 (Cav1) mediates the Midkine (MK)-induced Angiotensin I converting enzyme (ACE) expression contributing to epithelial-mesenchymal transition (EMT) in human lung epithelial cells (**Figure 6**).

2.3 Objectives

2.3.1 Objective 1

Investigate whether stimulation of human lung epithelial cells modulates ACE and EMT using two models:

1. Two-hit stimulation of HCl and mechanical stretch, and
2. Recombinant human MK.

2.3.2 Objective 2

Examine whether Notch family members interact with Cav1 leading to ACE signaling in human lung epithelial cells.

2.3.3 Objective 3

Investigate the role of Cav1 in the MK-Notch2-induced ACE and EMT signaling in human lung epithelial cells.

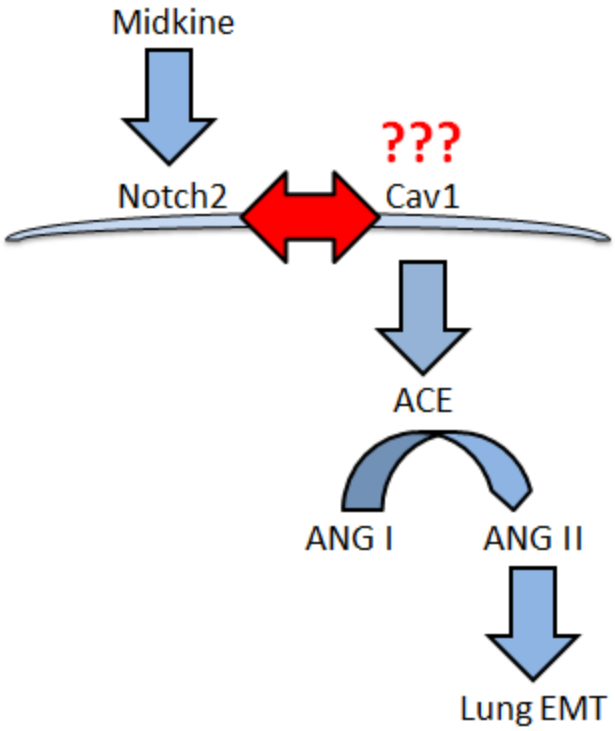

Figure 6. Hypothesis that Cav1 may mediate the MK-modulated ACE signaling in human lung epithelial cells.

Chapter 3
Methods

3.1 Materials

3.1.1 Antibodies

Rabbit α-human Angiotensin I converting enzyme pAb, rabbit α-human Caveolin1 pAb, rabbit α-human Midkine mAb, rabbit α-human Notch2 pAb, rabbit α-human α-Smooth muscle actin pAb, and rabbit α-human IgG pAb were purchased from Abcam® (Cambridge, England, UK). Rabbit α-human Notch1 mAb, rabbit α-human Notch3 mAb, and rabbit α-human IgG mAb were purchased from Cell Signaling Technology Inc.® (Beverly, MA, USA). Mouse α-human Notch4 mAb was purchased from Santa Cruz Biotechnology® (Dallas, TX, USA). Mouse α-human E-cadherin mAb, mouse α-human Cytokeratin8 mAb, mouse α-human Vimentin mAb, and mouse α-human IgG mAb were purchased from Cell Signaling Technology Inc.® (Beverly, MA, USA). Mouse α-human β-actin mAb was purchased from Sigma-Aldrich® (St. Louis, MO, USA). Goat α-rabbit IgG-HRP secondary antibody was purchased from Jackson ImmunoResearch Laboratories Inc. (Westgrove, PA, USA). Goat α-mouse IgG-HRP secondary antibody was purchased from Invitrogen-Thermo Fischer Scientific (Waltham, MA, USA).

3.1.2 Recombinant Protein

Recombinant human midkine was purchased from R&D Systems® (Minneapolis, MN, USA).

3.1.3 siRNA Transfection Reagents

DharmaFECT Transfection Reagent I, ON-TARGETplus Human Caveolin1 siRNA SMARTpool, and ON-TARGETplus Non-targeting Control siRNA were purchased from Dharmacon-Thermo Fisher Scientific (Waltham, MA, USA). Human Caveolin1 siRNA SMARTpool arrived as a mixture of four individual siRNA target sequences with enhanced potency and specificity for the Caveolin1 gene (**Appendix A**).

3.1.4 Cell Culture of Human Bronchial Epithelial Cells (BEAS-2B)

Human bronchial epithelial cells (BEAS-2B) were grown in 75 cm^2 flasks at a density of 2.1-8.4 x 10^6 cells/ml in Dulbecco's Minimal Essential Medium (DMEM) (Sigma Aldrich), supplemented with 10% fetal bovine serum (FBS) and 1% Penicillin/Streptomycin (P/S). Cells were washed with phosphate-buffered saline (PBS), trypsinized with 0.25% Trypsin-EDTA, neutralized with the same volume of DMEM, and centrifuged at 200 G-force for 6 minutes at 25°C. Cells were resuspended in DMEM, counted in a 1:2 diluted suspension using the Vi-CELL™ Cell Counter, and were re-plated in 6- or 24-well plates and incubated at 37°C at 5% CO_2 overnight prior to experiments.

3.2 *In Vitro* Models of ACE and EMT Signaling in Human Lung Epithelial Cells

3.2.1 Two-Hit Injury Model of Acid and Mechanical Stretch in Human Lung Epithelial Cells

BEAS-2B cells were seeded in 6-well Collagen Type I-coated BioFlex culture plates (Flexcell International, Hillsborough, NC, USA) at a density of 3.0 x 10^6 cells/well for PBS groups, and 3.3 x 10^6 cells/well for HCl groups (10% more cells to account for cell death due to acid treatment). After 24 hours, cells were exposed to 6.0 N HCl to reach pH 4.0 in serum-free

DMEM. Control groups were treated with the same volume of PBS as HCl in serum-free DMEM. Cells were treated with HCl or PBS for 30 minutes, washed with PBS two times, and cultured with DMEM containing 10% FBS and 1% P/S for 20 hours. Cells were washed with PBS and cultured in DMEM containing 0.1% FBS for 4 hours prior to mechanical stretch. Cells were subjected to cyclic mechanical stretch (20% elongation, 0.33 Hz or 20 cycles/min) using the Flexcell FX-5000 Tension System (Flexcell International, Hillsborough, NC, USA) for 24 hours. Cytotoxicity was measured using LDH assay. Western blot was used to detect MK protein expression.

3.2.2 Direct Injury Model of Stimulation with Recombinant Human Midkine (rhMK) in Human Lung Epithelial Cells

BEAS-2B cells were seeded in 24-well plates at a density of 0.75×10^5 cells/well and allowed to attach overnight. Cells were stimulated with 500 ng/ml of recombinant human MK (rhMK) or vehicle control PBS, and cells were washed to remove rhMK. Cells were collected at 48 hours after stimulation. Cytotoxicity was assessed by LDH assay. Protein expression of ACE and EMT markers, Vimentin and E-cadherin, were determined by Western blot. MK, Notch2, and Cav1 expression were also assessed by Western blot.

3.3 Co-Immunoprecipitation Assays for Cav1 and Notch 1, 2, 3, and 4

BEAS-2B cells were seeded in 75 cm^2 flasks and allowed to attach and grow until 80% confluency was reached. Flasks were washed with PBS and whole cell lysates were collected using 1 ml lysis buffer per flask. For each group, 500 μg of total protein was topped up to 1 ml with PBS, and were incubated with 1 μg of Notch1 mAb, Notch2 pAb, Notch3 mAb, Notch4

mAb, Cav1 pAb, or IgG mAb or pAb on a rotator overnight at 4°C. Each sample was incubated for 2 hours at room temperature with Protein A/G bead slurry (30 µl) (Protein AG UltraLink Resin, Thermo Scientific). Samples were centrifuged at 8,000 rpm (Microcentrifuge 5415 D, Eppendorf, Mississauga, ON, CA) for 1 minute at room temperature to precipitate Protein A/G beads. The supernatant was removed from each tube, and samples were washed two times in high-salt HNTG buffer (500 mM NaCl, 20 mM Hepes, 10% glycerol, 0.1% Triton X-100, pH 7.5) and three times in low-salt HNTG buffer (150 mM NaCl, 20 mM Hepes, 10% glycerol, 0.1% Triton X-100, pH 7.5). Proteins were eluted from the beads with 50 µl of 1x loading buffer and were boiled at 99°C for 5 minutes. Western blot was run using a SDS/10% polyacrylamide gel as described in Section 3.6, to visualize Cav1, Notch 1, Notch2, Notch3, and Notch4 expressions. Co-immunoprecipitation assays for Cav1 and Notch2 were repeated a total of 10 times. Co-immunoprecipitation assays for Cav1 and Notch1, 3, and 4 were repeated 4 times.

3.4 Cav1 siRNA Transfection in Human Lung Epithelial Cells

3.4.1 Cav1 siRNA Transfection in Human Lung Epithelial Cells

BEAS-2B cells were seeded in 24-well plates at a density of 0.75 x 10^5 cells/well and allowed to attach overnight. Cells were mixed with 1 µl of DharmaFECT Transfection Reagent I with 49 µl of OptiMEM per well. The solution of DharmaFECT Transfection Reagent I and OptiMEM were mixed with a pool of 50 nM of Cav1 siRNA or scrambled siRNA as control and DMEM without FBS or P/S was added to the siRNA solution make a final volume of 0.5 ml per well. BEAS-2B cells were transfected for 24 hours, then cells were washed with PBS and replaced with fresh DMEM with 10% FBS and 1% P/S for an additional 24 hours. Cells were collected at 48 hours

from the start of transfection. Cytotoxicity was assessed by LDH assay, and Cav1 and ACE protein expression was determined by Western blot.

3.4.2 Cav1 siRNA Transfection in the Presence or Absence of rhMK Stimulation

BEAS-2B cells were seeded in 24-well plates at a density of 0.50 x 10^5 cells/well and allowed to attach overnight to reach 30% confluency. Cells were transfected with 50 nM Cav1 siRNA or scrambled siRNA for 48 hours as described in Section 3.4 to reach 70% confluency. Next, wells were washed with 0.5 ml/well PBS and were stimulated with 500 ng/ml rhMK or PBS, and cells were washed to remove rhMK as described in Section 3.2.2. After the full experiment, cells were at full confluency, and the culture medium and total cell lysates were collected at 96 hours for analyses. Cell cytotoxicity was measured and expression of MK, Notch2, Cav1, and ACE were determined by Western blot.

3.5 Optimizations for rhMK Stimulation and Cav1 siRNA Transfection

3.5.1 rhMK Stimulation Optimization

BEAS-2B cells were seeded in 24-well plates at a density of 0.75 x 10^5 cells/well and allowed to attach overnight. Cells were stimulated with varying concentrations of rhMK (100 ng/ml, 250 ng/ml, 500 ng/ml, or 1,000 ng/ml) or vehicle control PBS at 24 and 48 hours, to assess cytotoxicity and optimize the dose and time of rhMK stimulation. Cytotoxicity was assessed by LDH assay. Protein expression of ACE and EMT markers Vimentin and E-cadherin were determined by Western blot. For the rhMK stimulation, a final optimized dose of 500 ng/ml was used for 48 hours.

3.5.2 Cav1 siRNA Transfection Optimization

Cells were mixed with 1 µl of DharmaFECT Transfection Reagent I with 49 µl of OptiMEM per well. The solution of DharmaFECT Transfection Reagent I and OptiMEM were mixed with 50 nM or 100 nM of Cav1 siRNA or scrambled siRNA as control and DMEM without FBS or P/S was added to the siRNA solution make a final volume of 0.5 ml per well. BEAS-2B cells were transfected for 24 hours, then cells were washed with PBS and replaced with fresh DMEM with 10% FBS and 1% P/S for an additional 24 hours. Cytotoxicity was assessed by LDH assay and Cav1 expression was determined by Western blot. The optimized concentration and time was 50 nM siRNA for 24 hours, and cells were collected after a total of 48 hours from the start of transfection.

3.6 Western Blot

3.6.1 Sample Preparation

Following each experiment, culture medium from different treatment groups were collected and stored at -80°C for future use. Cells were placed on ice, washed with PBS (1 ml/well for 6-well plates, and 0.5 ml/well for 24-well plates), and were lysed with lysis buffer (50-100 µl/well). Lysis buffer consisted of 150 mM NaCl, 50 mM Tris-HCl, 2 mM EDTA, 2 mM EGTA, 1% Triton X-100, 1% phosphatase inhibitor Na_3VO_4, and 1% proteinase inhibitor cocktail (Thermo Scientific), pH 7.54. Cells were scraped from the wells thoroughly, collected in 1 ml Eppendorf tubes, and incubated on ice for 5-10 minutes prior to centrifugation. The cell lysates were centrifuged at 16,000 G-force for 15 minutes at 4°C, and supernatants were collected into new Eppendorf tubes and stored at -80°C for future use.

Protein concentration was measured using a 96-well plate loaded with total cell lysate samples and a protein standard. The protein standard was prepared by serial dilution of bovine serum albumin (BSA) (Sigma-Aldrich, St. Louis, MO, USA) in double distilled water to produce final concentrations of 0.0625, 0.125, 0.25, 0.5, 1.0, and 2.0 mg/ml. A volume of 10 µl protein sample or standard was added to 150 µl Protein Assay Reagent (Pierce, Rockford, IL, USA) and incubated for 5-10 minutes at room temperature. The plate was read at an absorbance of 660 nm using spectrophotometry (SpectraMax 340, Molecular Devices) and protein concentrations of samples were calculated using the standard curve.

For co-immunoprecipitation assays, 50 or 500 µg of total protein was used with 6X loading buffer. For regular Western blots, 25 or 50 µg of total protein was diluted in 6X loading buffer. Loading buffer was composed of 375 mM Tris-HCl, 48% glycerol, 9% MeSH, 6% SDS, 0.03% β-mercaptoethanol, pH 6.8. Samples were denatured at 99°C for 5 minutes, placed on a rack at room temperature for 5 minutes until loading onto gels.

3.6.2 Gel Electrophoresis and Transfer

Samples and the molecular weight marker (6 µl at the front, 3 µl at the back) (BioRad, San Diego, CA, USA) were loaded onto 8, 10, or 12% SDS-polyacrylamide gels. A one-dimensional gel electrophoresis system (BioRad, San Diego, CA, USA) was used with 1X running buffer (192 mM glycine, 25 mM Tris-HCl, and 0.1% SDS). A constant voltage of 85 V was applied for the first 15 minutes to allow proteins to level at the stacking gel, followed by an increased voltage to 120 V for 1.5 hours until proteins reached the bottom of the gel.

A wet transfer system (BioRad, San Diego, CA, USA) was used to transfer proteins onto a 0.4-μm pore nitrocellulose membrane. A constant current of 350 mA was applied for 2.5 hours to ensure all proteins migrated to the membrane.

3.6.3 Immunoblotting

Following transfer, the nitrocellulose membranes were blocked with 5% milk in TBS-T (1.5 M NaCl, 0.5 M Tris, pH 7.4, 0.1% Tween-20) for 1 hour at room temperature on a shaking device. Each membrane was briefly rinsed with TBS-T, cut into various pieces at the appropriate molecular weight, and incubated in primary antibody solutions for 1 hour at room temperature, or overnight at 4°C. Primary antibody solutions were prepared in 5% BSA in TBS-T with the following dilutions: MK mAb (1:500), Notch2 pAb (1:10,000), Cav1 pAb (1:10,000), ACE pAb (1:2,000), β-actin mAb (1:1,000), α-SMA pAb (1:1,000), Notch1 mAb (1:1,000), Notch3 mAb (1:1,000), and Notch4 mAb (1:1,000). Membranes were washed for 10 minutes three times in TBS-T, we incubated in appropriate secondary antibody solutions (1:5,000 or 1:10,000) in 5% milk at room temperature. Finally, membranes were washed for 10 minutes three times with TBS-T and enhanced chemiluminescence solution was added for up to 1 hour to visualize bands.

3.7 Endpoints

3.7.1 Cytotoxicity (LDH)

After each experiment, culture medium (0.5 to 1.5 ml) was collected from stimulated BEAS-2B cells. Supernatants were centrifuged at 16,000 G-force for 15 minutes at 4°C, aliquoted into fresh tubes, and stored at -80°C until used for measurements.

Cell cytotoxicity was measured using the Cytotoxicity Detection Kit (LDH) (Roche Applied Science, Penzberg, Germany). Lactate dehydrogenase (LDH) enzyme activity in the cell culture medium increases with a rise in the number of dead cells, or cells with a damaged plasma membrane. This colorimetric assay quantifies cell injury and death based on LDH conversion of lactate to pyruvate by reducing NAD+ to NADH. Diaphorase uses NADH to reduce a tetrazolium salt (INT) to a red formazan product, which is directly proportional to LDH released. In the LDH assay, 100 µl of sample was incubated with 100 µl of reagent in a 96-well plate for 10-30 minutes, and the plate was read at 490 nm absorbance by the spectrophotometer.

In each experiment, a well was used for the "low control" (LC) group and a "high control" (HC) to calculate percent cytotoxicity. The LC group comprised of BEAS-2B cells in culture medium with no treatment. The HC group also received no treatment, however, 2% Triton X-100 in the same volume of medium was used to lyse cells at the end of each experiment. The LC optical density (OD) value was used as the baseline cytotoxicity, and the OD value of the HC was used as 100% or maximum cytotoxicity.

The formula to calculate percent cytotoxicity as given by Roche Applied Science is as follows:

$$\%\ Cytotoxicity = \frac{Sample\ OD\ value - LC\ OD\ value}{HC\ OD\ value - LC\ OD\ value}$$

3.7.2 MK, Notch2, Cav1, and ACE Protein Expression

Protein expression of MK, Notch2, Cav1, and ACE were determined by Western blot as described in Section 3.6. Once the protein bands were obtained on the films with chemiluminescence, the films were scanned using the GS-800^{TM} Calibrated Densitometer

(BioRad, San Diego, CA, USA). Quantification analyses were performed using Quantity One software associated with the scanner, or with ImageJ software. All raw data were normalized with β-actin, and the normalized values were graphed using GraphPad Prism v.6.00c (GraphPad Software Inc., San Diego, CA, USA).

3.7.3 EMT Markers

Protein expression of EMT markers, E-cadherin Cytokeratin8, Vimentin, and α-SMA were determined by Western blot as described in Section 3.6. The EMT markers were quantified and analyzed in a similar manner to target proteins of interest.

3.7.4 Soluble ACE in Culture Supernatant

Soluble ACE measurements were performed using an ACE enzyme-linked immunosorbent assay (ELISA) kit provided by Abcam® (Cambridge, England, UK). Wells pre-coated with monoclonal ACE capture antibody were provided. Briefly, standards and samples were added into wells, after which wells were incubated with biotinylated anti-human ACE. To detect soluble ACE in the "very low target concentration" range of <156 pg/ml, the cell culture supernatant samples were not diluted. Following incubation, a PBS buffer was used to wash the plate, and an Avidin-Biotin-Peroxidase Complex was added. Following incubation, unbound conjugates were removed by washing with PBS buffer, and the TMB Color Developing Agent was added into each well to visualize the HRP reaction. After 45 minutes, TMB Stop Solution was added and the plate was read immediately at 450 nm.

3.8 Statistical Analyses

Statistical analyses were performed using GraphPad Prism v.6.00c (GraphPad Software Inc., San Diego, CA, USA). All data in the figures are presented as mean ± standard error, and a p-value equal to or less than 0.05 was deemed as statistically significant. Statistical significance was determined by a two-tailed independent t-test, or a two-way ANOVA followed by a Tukey post-hoc test.

Chapter 4
Results

4.1 Objective 1 – Investigate Whether Stimulation of Human Lung Epithelial Cells Modulates Angiotensin I Converting Enzyme and Epithelial-Mesenchymal Transition

4.1.1 Two-Hit *In Vitro* Model Induces Midkine Expression in Human Lung Epithelial Cells

We observed upregulation of MK expression in our previously established a two-hit *in vitro* model of ARDS by HCl and mechanical stretch. HCl was used to mimic ARDS-associated aspiration pneumonitis, which attributes to 30% mortality in ARDS [144]. Mechanical stretch was used to reproduce the features of mechanical ventilation in ARDS patients [32]. BEAS-2B cells were stimulated with HCl (pH = 4.0) or PBS for 30 minutes, followed by mechanical stretch (MS) at 20% elongation at a frequency of 0.33 Hertz (20 cycles/min) or static conditions (C) for 24 hours (**Figure 7A**).

Prior to investigation of protein expression in our two-hit injury model, LDH assay was performed to measure cell cytotoxicity following each experiment. There was no significant increase in LDH release following HCl or MS, with a maximum of 1% cytotoxicity in the HCl + MS group (**Figure 7B**). Next, Western blot was performed to determine MK protein expression in our model. We found that exposure of human lung epithelial cells to HCl did not upregulate MK expression, however, MS with or without HCl showed a significant upregulation in MK ($p < 0.0099$, $N = 4$) (**Figure 7C**). Thus, HCl alone did not have much effect on MK expression, however, MS alone or MS + HCl resulted in a significant upregulation of MK expression.

Thus, we demonstrated that MK expression was induced in our two-hit *in vitro* model of HCl and mechanical stretch. Next, we wanted to examine the downstream signaling of ACE and EMT that is specifically induced by MK. Recombinant human MK (rhMK) synthesized by E.*coli* was used to examine the role of MK in lung epithelial cells in a specific manner. In the next experiments, rhMK was used to stimulate BEAS-2B cells in order to investigate the MK-Notch2 induced ACE and EMT signaling pathway.

4.1.2 Recombinant Human Midkine Stimulates Human Lung Epithelial Cells

Various doses and time points for rhMK were used for optimal stimulation of lung epithelial cells. BEAS-2B cells were stimulated with 100 ng/ml, 500 ng/ml, and 1,000 ng/ml rhMK or PBS for 24 and 48 hours (**Figure 8A**). The rhMK was washed out after 24h of stimulation, and the protein expressions were measured from cell lysate. ACE, E-cadherin, and Vimentin protein expressions were examined as the endpoints to determine the final concentration and time point of rhMK (**Figure 8B**). The experiment was repeated five times to obtain the final optimal dose of 500 ng/ml rhMK for 48 hours.

4.1.3 Recombinant Human Midkine Upregulates ACE and Mesenchymal Marker Expression

Previously, it has been demonstrated that MK may act as a novel regulator of ACE in human microvascular endothelial cells [62], however, this has not been confirmed specifically in human lung epithelial cells. Several groups have shown that MK promotes EMT *in vivo* and *in vitro* [64, 65, 145]. BEAS-2B cells were stimulated with 500ng/ml rhMK or PBS control for 48 hours, and MK, ACE, E-cadherin, Vimentin, Cav1, and Notch2 expressions were determined by Western blot (**Figure 9**).

MK expression was measured in endogenous cell lysates of lung epithelial cells. Stimulation of lung epithelial cells with rhMK upregulated endogenous MK expression (1.000 ± 0.3457 vs. 5.254 ± 0.2727, N= 3, p= 0.0006). Furthermore, there was a significant increase in ACE expression following stimulation of BEAS-2B with rhMK compared to the PBS control group (1.000 ± 0.1856 vs. 1.713 ± 0.2218, N= 4, p= 0.0487).

EMT was investigated in BEAS-2B by detection of E-cadherin (epithelial marker) and Vimentin (mesenchymal marker). Interestingly, there was no significant change in E-cadherin expression (1.000 ± 0.09859 vs. 0.8178 ± 0.08675, N= 4, p= 0.2147), however, there was a significant increase in Vimentin expression (1.000 ± 0.2153 vs. 1.726 ± 0.3193, N= 5, p=0.0525) in the rhMK stimulated group compared to the PBS control group (**Figure 9**). These results demonstrate that MK may induce the upregulation of mesenchymal marker expression in lung epithelial cells.

There was no significant change in expression of the transmembrane proteins, Notch2 (1.000 ± 0.07847 vs. 0.9841 ± 0.1576, N= 4, p= 0.9311) or Cav1 (1.000 ± 0.09484 vs. 1.054 ± 0.1122, N= 4, p= 0.6504) in the rhMK-stimulated group compared to the PBS control group (**Figure 9**).

Our experiments confirmed that MK expression is induced upon two-hit stimulation of HCl and mechanical stretch. Furthermore, we demonstrated that stimulation with rhMK upregulates ACE and mesenchymal marker expression in lung epithelial cells.

The complete blots for the rhMK stimulation optimization experiment in **Figure 8** are shown in **Supplementary Figure 1**.

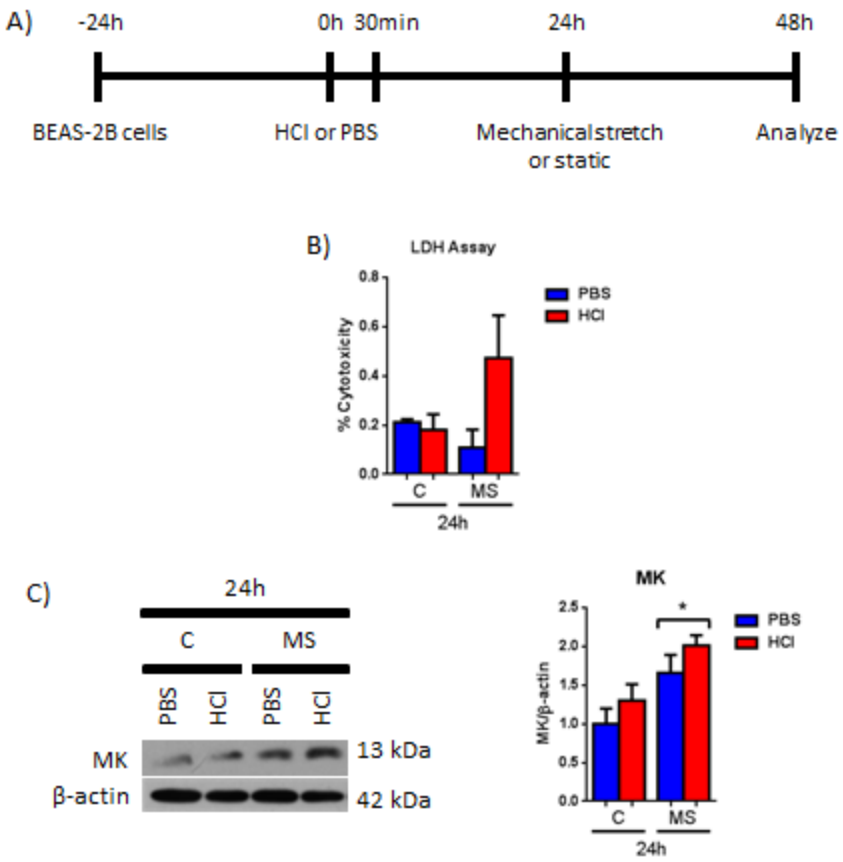

Figure 7. MK expression is upregulated in a two-hit *in vitro* model of HCl and mechanical stretch. A) BEAS-2B cells were seeded in 6-well Flexcell plates coated with collagen I and allowed to attach overnight. BEAS-2B cells were stimulated with HCl (pH = 4.0) or PBS control for 30 minutes, followed by mechanical stretch at 20% elongation at a frequency of 0.33 Hertz (20 cycles/min)for . B) LDH assay on BEAS-2B cells after HCl and mechanical stretch shows less than 1% cytotoxicity, suggesting that cells are still viable. C) Western bot was performed to determine MK expression. After HCl, MK expression was not significantly upregulated, but with mechanical stretch there was a signficant upregulation of MK expression. * $p < 0.05$ vs. C 24h; N = 4. C= Static; MS= Mechanical stretch; Blue = PBS; Red = HCl. Error bars represent standard error of the mean.

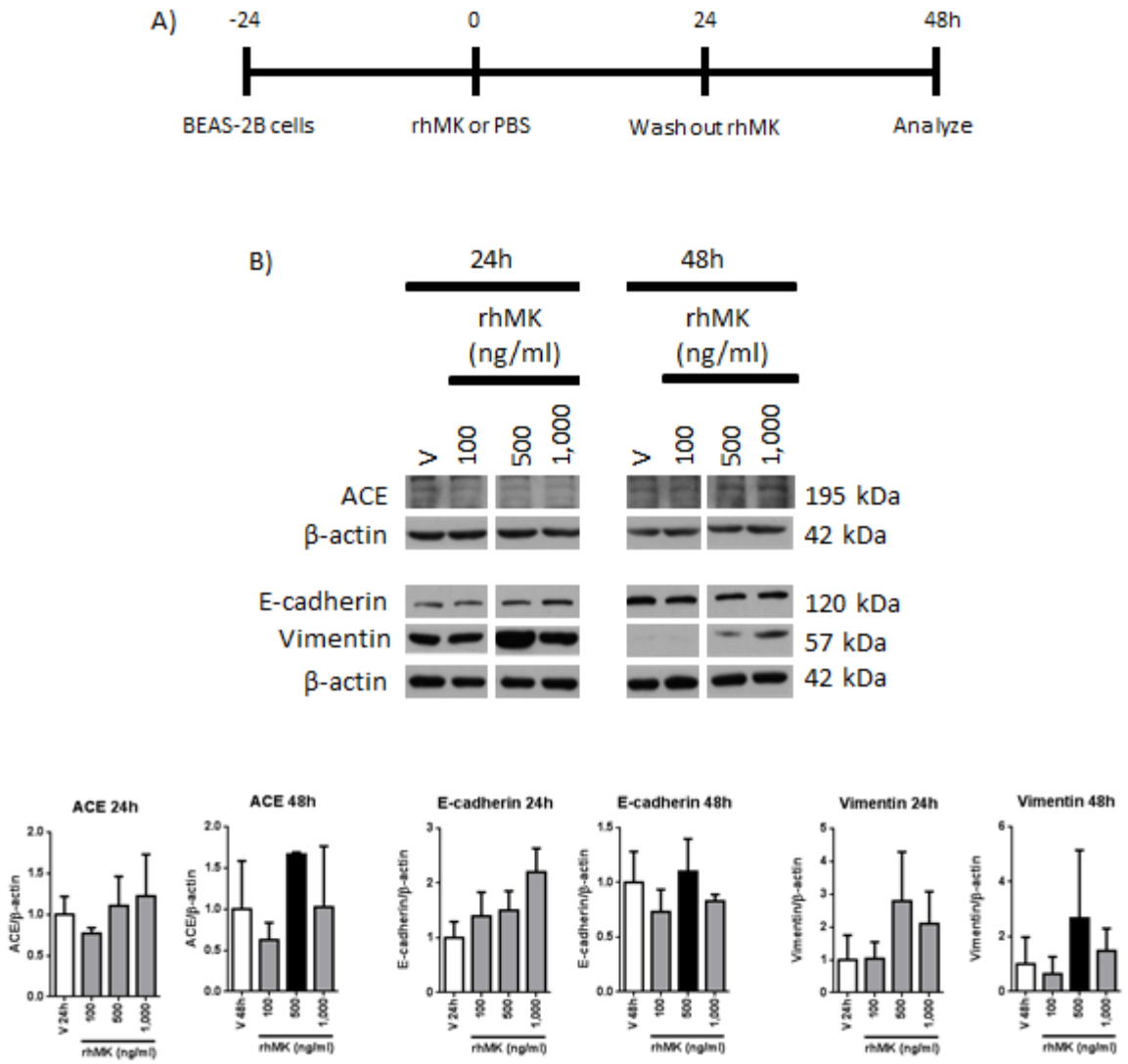

Figure 8. Recombinant MK (rhMK) stimulation of BEAS-2B cells with various doses and time points to determine ACE and EMT signaling. A) BEAS-2B cells were seeded on 24-well plates and were stimulated with 100, 500, and 1,000 ng/ml rhMK or PBS control for 24 and 48 hours. B) Whole cell lysates were collected and Western blot was run to detect ACE, E-cadherin, and Vimentin. BEAS-2B stimulation with 500 ng/ml rhMK for 48 hours exhibited the optimal conditions to activate ACE expression and induce EMT. The experiment for 24 and 48 hours was performed 2 times in pooled triplicates. V = Vehicle control. White bar = Vehicle control; Black bar = Final optimized dose; Grey bar = Stimulation optimization doses.

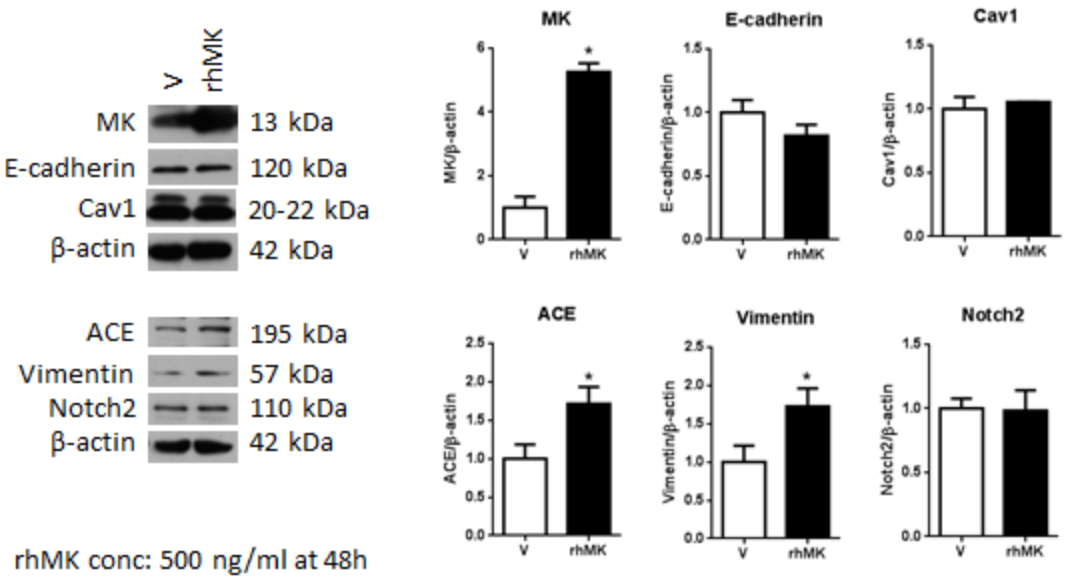

Figure 9. rhMK upregulates ACE and mesenchymal marker expression in human lung epithelial cells. BEAS-2B cells were seeded on 24-well plates and 24 hours later, cells were stimulated with PBS or the optimal dose of 500 ng/ml rhMK for 48h. Whole cell lysates were collected and protein expression was determined via Western blot. Experiment was performed 5 times in pooled triplicates. V = PBS. * $p < 0.05$ vs. V. Error bars represent standard error of the mean.

4.2 Objective 2 – Examine Whether Notch Family Members Interact with Caveolin1 in Human Lung Epithelial Cells

4.2.1 Notch1, 2, 3, and 4 in Human Lung Epithelial Cells

Since Notch and Cav1 proteins are both present at the plasma membrane, we examined their interaction in lung epithelial cells. Before investigating whether Cav1 may interact directly with Notch family members, Notch1, Notch2, Notch3, and Notch4 protein expressions were first assessed to confirm their expression in lung epithelial cells. The input control lane for each blot was probed with the targeted antibody for Notch1, 2, 3, and 4 respectively (**Figure 10**). The band in each blot confirmed that all four homologues of the Notch family are expressed in lung epithelial cells.

4.2.2 Caveolin1 Binds Specifically with Notch2

Co-immunoprecipitation assays were conducted to determine whether there is an interaction between Cav1 and the Notch homologues (**Figure 10**). Cav1 antibody was added to BEAS-2B whole cell lysate, followed by Protein A/G beads. The beads allowed the precipitation of the protein complex to be analyzed by Western blot. To confirm specificity of the interaction, Notch1, Notch2, Notch3, and Notch4 antibodies were added to BEAS-2B whole cell lysate, followed by addition of Protein A/G beads which were added to precipitate the protein complex in order to examine protein expression via Western blot.

In the Cav1 and Notch2 co-immunoprecipitation experiment, the input control lane showed that both Cav1 and Notch2 are expressed in lung epithelial cells. In the Notch2 immunoprecipitation

group, Cav1 and Notch2 proteins were both pulled down. Furthermore, in the Cav1 immunoprecipitation group, Cav1 and Notch2 proteins were both pulled down. The IgG immunoprecipitation group served as the negative control. These results suggest that there is a specific interaction of Cav1 and Notch2 in lung epithelial cells.

However, other Notch family members- Notch1, Notch3, and Notch4- each pulled down the corresponding Notch protein but it did not pull down Cav1. Cav1 immunoprecipitation groups also did not pull down Notch1, Notch3, or Notch4.

These results suggest that Cav1 binds specifically with Notch2, but does not bind with other Notch homologues, Notch1, Notch3, and Notch4 in lung epithelial cells.

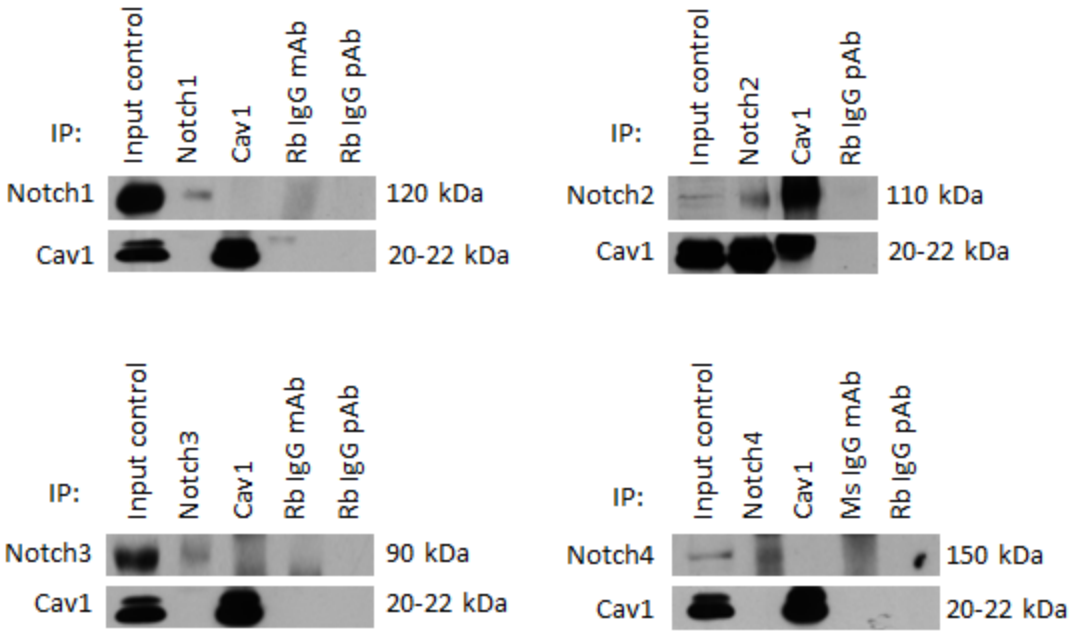

Figure 10. Cav1 binds specifically with Notch2, but not with homologues Notch1, 3, or 4 in lung epithelial cells. BEAS-2B whole cell lysates were used for the co-immunoprecipitation analyses. For each antibody, 1 µg Notch1 mAb, Notch2 pAb, Notch3 mAb, or Notch4 mAb were used as the bait. 1 µg Cav1 pAb was used to ensure its specificity with the Notch homologues. Corresponding rabbit and mouse IgG mAb and IgG pAb were used as negative controls. Co-immunoprecipitation was detected by Western blot in 500 µg total cell lysates. Experiments were performed 10 times for Cav1 and Notch2, and 4 times for Cav1 with Notch1, Notch3, and Notch4. IP = Immunoprecipitation.

4.3 Investigate the Role of Caveolin1 in the Midkine-Notch2-induced ACE and EMT Signaling in Human Lung Epithelial Cells

4.3.1 Caveolin1 is Significantly Knocked Down by siRNA Transfection

To assess the specific role of Cav1 on the MK-Notch2-ACE signaling pathway in lung epithelial cells, Cav1 was knocked down through siRNA transfection. For efficient transfection, 1 µl of DharmaFECT Transfection Reagent I was used for BEAS-2B cells in 24-well plates, as recommended by the DharmaFECT siRNA Transfection Protocol.

Cav1 knockdown was optimized in BEAS-2B whole cell lysates using a concentration of 50 nM Cav1 siRNA or scrambled siRNA control at 24 and 48 hours. Following each transfection experiment, Cav1, ACE, and Vimentin protein expressions were analyzed via Western blot (**Figure 11**). Transfection with Cav1 siRNA resulted in a clear reduction of Cav1 expression compared to the scrambled siRNA control group. A decrease in ACE expression was also observed in the Cav1 siRNA transfected group compared to the scrambled siRNA control group at 48 hours. Therefore, 50 nM siRNA at 48 hours was used as the optimized condition to continue further with this study.

4.3.2 Caveolin1 Knockdown Attenuates Notch2 and ACE Expression

Cav1 expression was sufficiently knocked down with 50 nM Cav1 siRNA at 48 hours, with a 67% decrease in protein levels compared to the scrambled siRNA group (1.000 ± 0.04814 vs. 0.3269 ± 0.03870, $N= 5$, $p< 0.0001$) (**Figure 12**).

Next, the key players of the pathway, Notch2 and ACE, were investigated for changes in protein expression. Interestingly, Notch2 expression was significantly decreased in Cav1 siRNA groups compared to scrambled siRNA control (1.000 ± 0.09930 vs. 0.3936 ± 0.07398, N= 4, p= 0.0027). Furthermore, there was a significant attenuation of downstream ACE expression in Cav1 siRNA transfected cells compared to scrambled siRNA (1.000 ± 0.1524 vs. 0.6004 ± 0.03909, N= 5, p= 0.0348).

4.3.3 Caveolin1 Knockdown Attenuates ACE and Mesenchymal Marker Expression in Recombinant Human Midkine-Stimulated Lung Epithelial Cells

Based on the results of Cav1 knockdown using siRNA transfection, lung epithelial cells were stimulated with rhMK following Cav1 knockdown to assess the role of Cav1 in the MK-Notch2-ACE pathway. BEAS-2B cells were transfected with 50 nM Cav1 siRNA or scrambled siRNA for 48 hours, followed by stimulation with 500 ng/ml rhMK or PBS for 48 hours. Protein expressions of Cav1, MK, Notch2, ACE, Cytokeratin8, α-SMA, and Vimentin were determined by Western blot (**Figure 10**).

First, Cav1 expression was determined to investigate its expression 96 hours after transfection. Cav1 expression was significantly reduced in the Cav1 siRNA + PBS group compared to the scrambled siRNA + PBS group (0.04544 ± 0.01658 vs. 1.000 ± 0.04322, N= 4, p<0.0001). Cav1 expression was also significantly decreased in the Cav1 siRNA + MK group compared to the scrambled siRNA + MK group (0.01617 ± 0.007743 vs. 0.8723 ± 0.05301, N= 4, p< 0.0001).

Next, endogenous MK expression was determined to confirm whether the lung epithelial cells were stimulated after a total of 96 hours. After 24 hours of rhMK stimulation, cells were washed out to remove rhMK, and MK expression was determined from cell lysate. The scrambled siRNA + MK group exhibited significantly high endogenous MK expression compared to the scrambled siRNA + PBS control group (19.94 ± 4.418 vs. 1.000 ± 0.1405, $N= 4$, $p<0.0052$), and similarly, the Cav1 siRNA + MK group showed a significant increase in MK expression compared to the Cav1 siRNA + MK group (15.72 ± 3.240 vs. 1.104 ± 0.5135, $N= 4$, $p<0.0043$). Thus, rhMK stimulation induced increased endogenous MK expression in human lung epithelial cells.

Next, downstream targets Notch2 and ACE were examined. Interestingly, there was no significant change in Notch2 expression. We no longer observed a reduction in Notch2 expression following Cav1 knockdown. However, ACE expression was significantly upregulated upon stimulation in the scrambled siRNA + MK group compared to the scrambled siRNA + PBS group (1.780 ± 0.2114 vs. 1.000 ± 0.1784, $N= 3$, $p<0.0478$) at 96 hours, similar to what was observed in the previous rhMK stimulation experiment at the 48 hour time point. Upon knockdown of Cav1 expression, a reduction in ACE expression was not observed as previously seen in the Cav1 knockdown experiment at the 48 hour time point. However, upon stimulation with rhMK, there was no longer an increase in ACE expression in the Cav1 siRNA + MK group compared to the Cav1 siRNA + PBS group (1.524 ± 0.2135 vs. 1.458 ± 0.2428, $N= 3$, $p=0.8481$). These results suggest that there may be a stabilization of Notch2 and ACE expression at 96 hours compared to the 48 hour time point in the Cav1 knockdown experiment. However, this requires further investigation.

Various EMT markers were used to determine whether Cav1 played an important role in epithelial cell transformation towards a mesenchymal phenotype upon rhMK stimulation. Cytokeratin8 was used to visualize epithelial marker expression. BEAS-2B cells did not exhibit a significant change in Cytokeratin8 expression in the Cav1 siRNA + PBS group compared to the scrambled siRNA + PBS group. However, upon rhMK stimulation, there was no significant change in the Cav1 siRNA + MK group compared to the scrambled siRNA + MK group.

Furthermore, mesenchymal markers, α-SMA and Vimentin, were used to visualize the mesenchymal phenotype transition of BEAS-2B cells. Again, there was no significant change detected upon Cav1 knockdown and/or rhMK stimulation in the mesenchymal markers. However, there was a visible trend towards an increase in α-SMA expression following rhMK stimulation of BEAS-2B cells, in the scrambled siRNA + MK group compared to the scrambled siRNA + PBS group. However, upon Cav1 knockdown followed by rhMK stimulation, there was a trend towards reduction in α-SMA expression in the Cav1 siRNA + MK group compared to the scrambled siRNA + MK group. In addition, Vimentin demonstrated trends similar to that of α-SMA expression upon Cav1 knockdown and rhMK stimulation. There was a visible increase in Vimentin expression in the scrambled siRNA + MK group compared to the scrambled siRNA + PBS group. However, upon Cav1 knockdown followed by rhMK stimulation, there was a clear trend towards a decrease in Vimentin expression in the Cav1 siRNA + MK group compared to the scrambled siRNA + MK group. Power analyses were performed to show that we may be able to detect difference between groups by increasing the sample size for each marker in future experiments.

Therefore, Cav1 knockdown attenuates Notch2 and ACE expression. However, the effect of Cav1 knockdown on ACE at 48 hours was no longer evident at the 96 hour time point. In addition, we observed a trend towards a reduction in mesenchymal marker expression in lung epithelial cells with Cav1 knockdown followed by rhMK stimulation.

The complete blots for the Cav1 siRNA transfection optimization experiment in **Figure 11** are shown in **Supplementary Figure 2.**

The complete blots for the Cav1 siRNA + rhMK stimulation experiment in **Figure 13** are shown in **Supplementary Figure 3**.

Soluble ACE in cell culture conditions for the Cav1 siRNA + rhMK stimulation experiment in **Figure 13** is shown in **Supplementary Figure 4**.

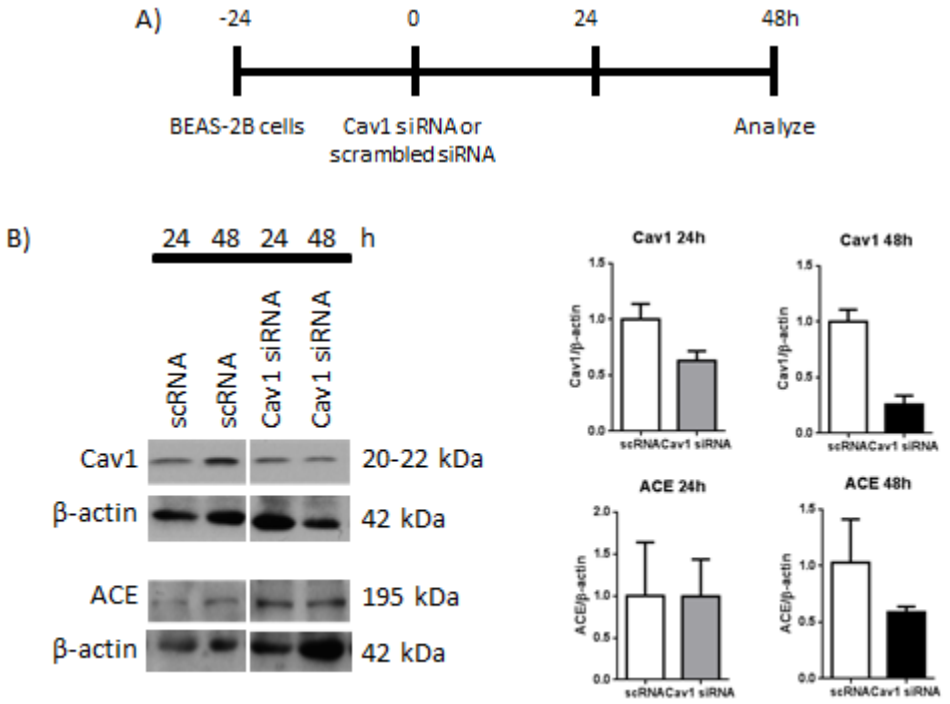

Figure 11. Cav1 siRNA transfection of BEAS-2B cells at various doses and time points to determine downstream ACE expression. A) BEAS-2B cells were seeded on 24-well plates and were stimulated with 50 and 100 nM Cav1 siRNA or scrambled siRNA control for 24 and 48 hours. B) Whole cell lysates were collected and Western blot was run to detect Cav1 and ACE protein expressions during transfection optimization. Transfection of BEAS-2B cells with 50 nM Cav1 siRNA for 48 hours exhibited the optimal condition to block ACE and EMT signaling. The experiment was conducted 2 times in pooled triplicates. scRNA = Scrambled siRNA; Cav1 siRNA = Caveolin1 siRNA; White bar = Scrambled siRNA control; Black bar = Final optimized transfection dose; Grey = Optimization transfection doses.

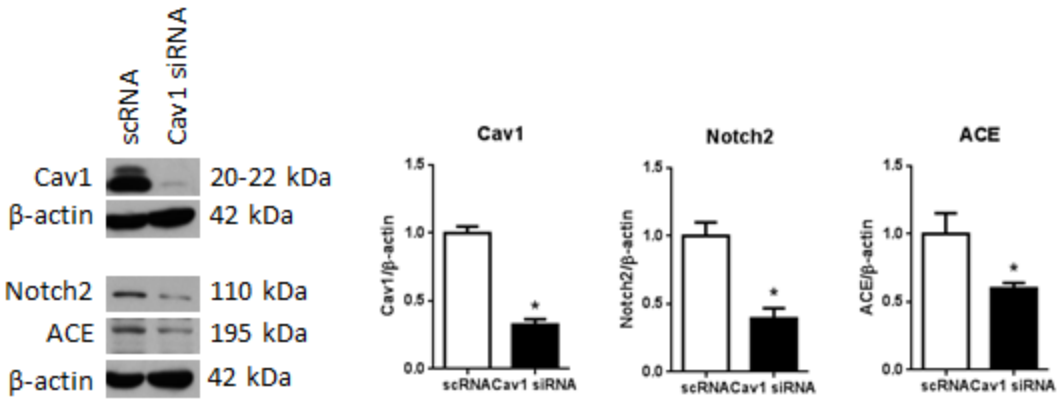

Figure 12. Cav1 knockdown attenuates Notch2 and ACE expression. BEAS-2B cells were transfected with Cav1 siRNA or scrambled siRNA control (50 nM) for 48 hours. The experiment was repeated 6 times in pooled triplicates. scRNA = Scrambled siRNA; Cav1 siRNA = Caveolin1 siRNA. * $p < 0.05$ vs. scRNA. Error bars represent standard error of the mean.

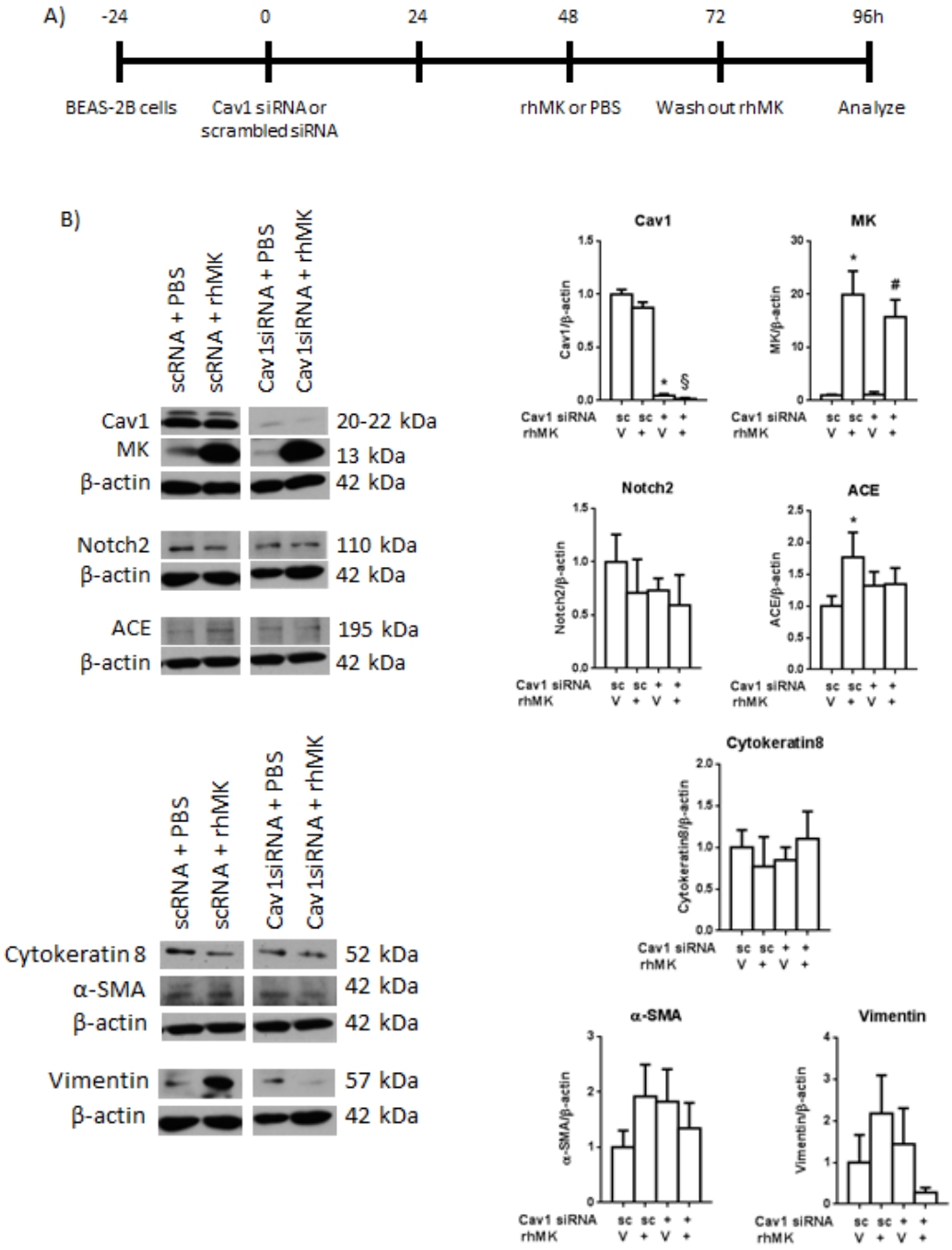

Figure 13. Cav1 knockdown attenuates the rhMK-induced ACE and mesenchymal marker expression in human lung epithelial cells. A) BEAS-2B cells were seeded, transfected with 50 nM Cav1 siRNA or scrambled siRNA control for 48 hours, and treated with 500 ng/ml rhMK or PBS control for another 48 hours. The time point at which samples were collected was 96 hours. B) Western blot was performed to determine protein expression. Experiments were performed 4 times in pooled triplicates. V = Vehicle control (PBS); scRNA = Scrambled siRNA; Cav1 siRNA = Caveolin1 siRNA. * $p < 0.05$ vs. scRNA + V; § $p < 0.05$ vs. scRNA + MK; and # $p < 0.05$ vs. Cav1 siRNA + V.

Chapter 5
Discussion and Future Directions

5-1 DISCUSSION

5.1 The Role of ACE in the Fibrotic Response in Lung Epithelial Cells

5.1.1 *In Vitro* Model Considerations

Although ACE is widely expressed in the lung epithelium, ACE is primarily found in the lung endothelium due to its major functions as a regulator of the vasculature. The renin-angiotensin system is highly active in the lung and it is therefore not surprising that pulmonary endothelial cells would possess higher ACE expression. Our group and others have shown that ACE is indeed present in bronchial epithelial cells (BEAS-2B) and in adenocarcinoma alveolar basal epithelial cells (A549). Many studies use BEAS-2B and A549 cells to investigate pulmonary physiology and pathophysiology in the *in vitro* setting [146-148]. In addition, our previous findings of EMT signaling via the MK-Notch2-ACE pathway in BEAS-2B cells have been confirmed also in A549 cells. Therefore, this investigation was carried out in BEAS-2B cells to examine the molecular mechanisms of EMT via activation of ACE expression. Our findings may translate quite well due to the more potent expression and activity of ACE in microvascular endothelial cells. Currently, the experiments in this thesis are being replicated in lung endothelial cells to confirm the findings in this study.

5.1.2 Significance of Increased ACE Expression

In normal physiology, ACE exerts 90% of its functions within the lung, which mainly comprise of exerting its role of cleaving Angiotensin I to the active product Angiotensin II. The renin-

angiotensin system regulates the systemic vasculature via Angiotensin II, but contributes a major role particularly in pulmonary and renal tissues. As a result, the lung and kidneys are the primary organs which are affected by the profibrotic signaling of ACE and other components of the renin-angiotensin system such as Angiotensin II. Angiotensin II is a widely established molecule involved in the development of pulmonary fibrosis. Since ACE generates Angiotensin II in the lung, increased activation of ACE expression suggests an elevation in metabolic activity of the ACE enzyme. Thus, we can conclude that ACE activation may result in increased concentrations of Angiotensin II. Furthermore, the renin-angiotensin system components, ACE and Angiotensin II, have been demonstrated to modulate EMT to promote fibrotic remodeling in ARDS-associate pulmonary fibrosis.

5.2 The Role of EMT in Human Lung Epithelial Cells

As previously discussed, EMT is a widely established hallmark of fibrotic remodeling in pulmonary fibrosis which may be induce by VILI. EMT is one of the major cellular sources of pulmonary fibrosis, and is characterized by the transformation of epithelial cells to a mesenchymal phenotype. EMT is mediated by changes in signaling of underlying cytoskeletal and adherent junction proteins to induce a loss of polarity and gain of invasiveness and migration. The most prominent epithelial markers are E-cadherin and Cytokeratin8, which were studied in our experiments. Vimentin and α-SMA are widely used to detect mesenchymal marker expression.

During lung injury, the lung epithelium is a major area of focus because alveolar Type I and Type II cells are the main components which carry out respiratory functions. Upon injury, the

lung epithelial cells may undergo EMT and invade into the interstitium to secrete ECM molecules as fibroblast-like cells. Therefore, EMT is an important process in the context of pulmonary fibrosis and requires extensive investigation. It is through the elucidation of the molecular mechanisms leading to activation of EMT that may uncover potential therapeutic targets for fibrosis.

Traditionally, EMT has been strictly characterized by the downregulation of epithelial markers and upregulation of mesenchymal markers. However, recent studies have described a new phenomenon of "tumor budding" in the context of cancer metastasis. Tumor budding is defined by the presence of clusters of undifferentiated malignant cells in the tumor stroma in close proximity of the invasive front of a tumor [149]. Recent studies support the phenomenon of tumor budding in the clinical setting, and it has further been shown as an independent prognostic of poor outcome in patients [150]. Tumor budding exhibited by partial EMT may also pose a higher risk in patients [151]. However, tumor budding has not yet entered routine clinical assessment due to lack of consensus on its exact definition, methodology of assessment, and the optimal way it can be used to classify prognosis in patients. Since tumor budding is a new concept, further evidence may be required to change the traditional view of EMT.

Interestingly, partial EMT in epithelial cells in the intermediate transitional phase can be characterized by weak cell-cell adhesion and collective cell migration. Because they share properties of both epithelial and mesenchymal cells, partial EMT cells may have either complete upregulation or complete downregulation of both epithelial and mesenchymal marker expressions. Although it is not known whether partial EMT may exist in the context of

pulmonary fibrosis and other tissue fibrotic diseases, it is a possible mechanism to explain an intermediate phenotype of epithelial or mesenchymal marker expression. Tumor budding and partial EMT are novel concepts that suggest that EMT is more complex than we had originally believed. Thus, these phenomena should be kept in interest for further examination in future studies.

5.3 *In Vitro* Models of Stimulation in Human Lung Epithelial Cells

5.3.1 Two-Hit Stimulation Model of HCl and Mechanical Stretch

Previously, we demonstrated that ARDS patients have elevated levels of MK expression in plasma samples within 24 hours of diagnosis. Furthermore, after initial injury to the lungs, ARDS patients are mechanically ventilated as support for respiration. Our two-hit injury model of HCl and mechanical stretch in human lung epithelial cells was used to induce MK expression. HCl was used in our model to mimic ARDS-associated aspiration pneumonitis, which attributes to 30% mortality in ARDS patients. Mechanical stretch was used to reproduce the features of mechanical ventilation in ARDS patients. In our model, there was no significant injury induced as measured by release of LDH. The cytotoxicity level of BEAS-2B cells was less than 1% in the two-hit group. However, our aim was not to induce cell cytotoxicity, which is suggestive of apoptosis, but rather, our objective was to stimulate lung epithelial cells to induce MK expression. Interestingly, MK was unchanged after stimulation with HCl, but mechanical stretch with or without HCl significantly upregulated MK expression. Thus, we were able to recapitulate the observed MK upregulation in the plasma of ARDS patients in an *in vitro* model. MK

expression was induced upon stimulation with mechanical stretch with or without HCl, and this provided validation for our use of rhMK in our next experiments.

5.3.2 Model of Direct Stimulation with Recombinant Human Midkine (rhMK)

We confirmed that MK expression was significantly upregulated in our two-hit *in vitro* model of HCl and mechanical stretch in human lung epithelial cells. Next, we developed a model of direct stimulation of BEAS-2B cells with rhMK. Since we have previously shown in our two-hit model that MK expression is upregulated, we stimulated lung epithelial cells with rhMK. It is possible that HCl and mechanical stretch may activate a number of other signaling pathways in the cell. Thus, we wanted to use rhMK to examine the pathway of ACE and EMT that was specifically induced by MK.

MK is a secreted growth factor and is therefore involved in autocrine regulation of cell signaling. MK mRNA and protein expressions have been shown to be highly elevated in pancreatic ductal adenocarcinoma cell lines, and this was further correlated with an increase in secretion of serum MK in cell culture supernatant [152]. Increased release of MK suggests that there is increased production of MK within the cell. We stimulated lung epithelial cells with rhMK and washed out the rhMK to remove any rhMK on cells. We then measured endogenous MK levels in cell lysate to determine protein expression. Our results demonstrated that rhMK stimulation of BEAS-2B cells in fact stimulated high endogenous MK production through autocrine signaling on itself. This novel finding supports the autocrine role of MK in a self-activating mechanism.

We used a concentration of 500 ng/ml rhMK for 48 hours in our experiment. Although cell culture systems cannot be directly translated to the clinical setting, we ensured to use a dose that was in a similar range to our previous findings in ARDS patients. Previously, we determined a significant upregulation of MK expression in human plasma of 18.0 ± 4.1 ng/ml in ARDS patients, compared to 5.3 ± 0.6 ng/ml MK in healthy individuals. Furthermore, the amount of secreted MK in circulating human plasma is most likely much lower in concentration compared to cellular levels. Thus, we believe that our optimal dose of 500 ng/ml rhMK is relevant to the clinical setting.

rhMK stimulation of BEAS-2B cells demonstrated a specific activation of the MK-Notch2-ACE signaling pathway with EMT. We observed a significant upregulation of ACE expression. Our data confirms that MK specifically induces ACE expression in lung epithelial cells. Furthermore, there was an increase in mesenchymal marker expression as shown by Vimentin. However, there was no change in the expression of the transmembrane proteins, Cav1 and Notch2. rhMK stimulation may not necessarily affect total Notch2 or Cav1 expression. Cav1 has several phosphorylation regions which may be activated upon stimulation. It has been reported in the literature that Cav1 phosphorylation is increased after mechanical stretch. Therefore, it is possible that their phosphorylation or activation may be changed upon stimulation. Furthermore, we determined protein expression of whole cell lysate, and not in separated fractions such as nuclear, cytosolic, and plasma membrane fractions. Since Cav1 and Notch2 are present at the plasma membrane, it is possible that their localization may change but this requires further investigation. In summary, our results suggest that MK may upregulate ACE and mesenchymal marker expression.

There is a limitation of using rhMK produced by host Escherichia coli, compared to purified human MK protein, which is that there may be differences in the post-translational modifications. rhMK is synthesized by inserting the human MK sequence into a plasmid and transfecting it into a host cell. The host takes up the DNA sequence undergoes normal transcription and translation to produce the final MK protein. Human proteins are subject to post-translational modifications by the human cellular machinery. However, post-translational modifications of proteins are not common in bacterial host machinery. Thus, a limitation of using Escherichia coli-synthesized rhMK may be that rhMK may not have similar post-translational modifications as MK produced by humans. This may impact the specificity of rhMK for other non-specific receptors and activation of downstream signaling. However, one major advantage of rhMK is that purified human protein is never 100% pure. Thus, purified MK may also have some contamination and may limit the specificity of signaling.

It has been demonstrated in literature that different forms of human MK exists, and the half-life of the MK protein is dependent on differential cleavage of the signal sequence [60]. The extended form of human MK, which has an additional sequence on its N-terminal, possesses a longer half-life. In humans, heparin-released MK in human plasma consists of 100% of the longer half-life MK product [153]. However, due to varying conditions and different cell stimulators, MK may have a different half-life. In Escherichia coli, rhMK is most likely the longer half-life form due to limited cleavage after translation of the protein.

5.4 The Role of Cav1 in the MK-Notch2-ACE Signaling Pathway in Lung Epithelial Cells

Cav1, the main component of a three-member family of Caveolins, form invaginations of the cell membrane called caveolae. Cav1 has been widely investigated as a major regulator of critical cellular processes such as cell proliferation, differentiation endocytosis, adhesion, migration, and plasma membrane protein distribution. Not surprisingly, Cav1 has recently emerged as a crucial molecule in disease context, such as EMT in tumor metastasis and lung injury. Cav1 has also been shown to regulate downstream ACE activity in the lung. However, the exact mechanism of Cav1 in regulating ACE and EMT still remains a major question in molecular biology. This study sheds light on a novel role of Cav1 in ACE and EMT signaling in human lung epithelial cells.

5.4.1 Cav1 Interacts Specifically with Notch2 in Lung Epithelial Cells

Cav1 has been demonstrated to interact with and sequester various cell surface signaling molecules through the Cav1 binding motif of the CSD. Cav1 binds to growth factors such as glycosyl phosphatidylinositol-linked proteins, Src-family tyrosine kinases, H-Ras, heterotrimeric G protein subunits, protein kinase C isoforms, and endothelial nitric oxide synthase.

Notch2 is a cell surface receptor widely implicated in development, and our group has previously demonstrated that MK binds to Notch2 to regulate EMT. Notch2 is a member of a family of 4 transmembrane proteins- Notch1, Notch2, Notch3, and Notch4, all of which possess highly conserved structure within the ECD, ICD, and the transmembrane domain. Although the Notch proteins possess an overall high degree of homology, a unique region called the TAD was identified in the ICD of Notch1 and Notch2. The Notch1 TAD consists of amino acids 2194-

2398 and the Notch2 TAD consists of amino acids 2154-2352, and is capable of activating transcription. Most importantly, the TAD region is not highly conserved in any of the Notch receptors, which makes it highly possible for the various ICDs to interact with different proteins and activate diverse gene transcription [83].

Previously, Notch ICD activation was viewed as a highly conserved mechanism of cleavage, activation, and its direct translocation from the plasma membrane across the cytosol into the nucleus to activate gene transcription. Studies have suggested that there may be a regulatory role of Cav1 on Notch2, however, no direct relationship has been established in literature [104, 143]. Interestingly, our study showed that Cav1 binds to Notch2, but not with Notch1, Notch3, and Notch4 in human lung epithelial cells. We speculate that this specific binding of Notch2 and Cav1 is attributed to the TAD region of Notch2, and the CSD region of Cav1. Our study therefore suggests a novel, direct interaction of Cav1 and Notch2 at the plasma membrane.

There is a limitation of using co-immunoprecipitation assays to examine the binding of Cav1 and Notch2. In a co-immunoprecipitation assay, it is possible that an antibody may pull down the targeted protein of interest which is bound to other non-specific proteins. Furthermore, there is also another possibility that the proteins of interest do not bind directly to each other, but in fact, could be mediated by a protein complex. As a result, co-immunoprecipitation assays cannot confirm direct binding of two proteins. Thus, we cannot conclude from our experiments that Cav1 and Notch2 have a direct interaction, but that it may associate through a protein complex. However, we can still conclude that Cav1 interacts specifically with Notch2, but not with other

Notch family members. Thus, our novel finding can be investigated further through specific binding assays.

5.4.2 Cav1 Regulates Notch2 and ACE Expression in Lung Epithelial Cells

Our study thus far has demonstrated that MK induces ACE and mesenchymal marker expression in lung epithelial cells. Furthermore, we have shown that MK binds to Notch2, which in turn interacts specifically with Cav1. Next, we want to investigate the role of Cav1 in lung epithelial cells.

First, Cav1 expression was knocked down using siRNA transfection. We achieved a significant reduction in Cav1 expression. Interestingly, we observed a significant decrease in Notch2 expression following knockdown of Cav1. We speculate that Notch2 expression is dependent on Cav1 expression, suggesting its crucial role in regulating Notch2 stability. Our results are supported by others which have shown that Cav1 knockdown in neural stem cells lead to a decrease in Notch. Through our study, we have clearly elucidated implicated direct relationship of Cav1 and Notch2, which exhibit a novel specific binding of these two transmembrane proteins.

Furthermore, we observed a significant decrease in ACE expression following Cav1 knockdown. An *in vivo* study by Maniatis *et al*. supports our findings by showing that Cav1 knockout mice exhibit a significant reduction in lung ACE activity and expression [141]. In addition, a study by Uyy *et al*. further supports our findings through overexpression of Cav1 which resulted in increased lung ACE activity [142]. This data confirms that Cav1 is an upstream regulator of

ACE expression in lung epithelial cells. Furthermore, Cav1 is required for Notch2 stability and expression through a direct binding mechanism.

5.4.3 Cav1 Knockdown Followed by rhMK Stimulation Attenuates ACE and Mesenchymal Marker Expression

Based on our time-dependent experiment of Cav1 knockdown, we combined the Cav1 siRNA transfection with rhMK stimulation. We were determined to find the role of Cav1 in rhMK stimulated lung epithelial cells to further investigate our proposed pathway. Cav1 knockdown using siRNA resulted in a significant reduction in Cav1 expression. In alignment with our rhMK stimulation experiment, we observed a significant upregulation of endogenous MK expression following rhMK stimulation in our full experiment. Interestingly, we no longer saw an effect on Notch2 expression following knockdown or stimulation. However, ACE was significantly upregulated upon rhMK stimulation, but knockdown of Cav1 expression also did not attenuate ACE expression, as we previously observed in the Cav1 knockdown experiment. Interestingly, ACE expression was no longer upregulated after rhMK stimulation in lung epithelial cells with Cav1 knockdown. These results suggest that Cav1 attenuates Notch2 and ACE expression, but this regulation may be dose- or time-dependent. Thus, further investigation is required to determine the role of Cav1 on both Notch2 and ACE.

In addition, we observed EMT markers following Cav1 knockdown and rhMK stimulation in lung epithelial cells. There was no change in the epithelial marker expression as shown by Cytokeratin8 following Cav1 knockdown and rhMK stimulation. We also observed two mesenchymal markers- Vimentin and α-SMA. Interestingly, there was a trend towards

upregulation of mesenchymal marker expression following rhMK stimulation. However, upon Cav1 knockdown and rhMK stimulation, there was a clear reduction in both Vimentin and α-SMA expression. Our data suggests that knockdown of Cav1 expression may regulate downstream mesenchymal marker expression, but this also requires further investigation.

In summary, our results demonstrate that knockdown of Cav1 expression attenuates Notch2 and ACE expression at 48 hours but not at the 96 hour time point with rhMK stimulation. Furthermore, it appears that Cav1 knockdown leads to a trend towards reduction in mesenchymal marker expression. Further investigation is required to determine the dose- and time-dependent effects of Cav1 on Notch2 and ACE expression.

A limitation of this study is that we observed atypical EMT marker expression throughout the study. Our previous work demonstrated a clear trend in EMT, with a downregulation of epithelial markers and upregulation of mesenchymal markers. However, our experiments did not exhibit clear EMT signal. In our rhMK stimulation experiment, we observed a clear upregulation in Vimentin expression; however, there was no change in E-cadherin. In our experiment with knockdown of Cav1 followed by rhMK stimulation, we observed a trend in Vimentin and α-SMA, but there was no change in Cytokeratin8. Atypical EMT marker expression may have been observed due to length of passage or source of cells. The cells may have transformed over time by culturing for a long duration of time. Furthermore, our laboratory received a new batch of cells and there was a visible difference in cell morphology and size between the cells that were used for this study and the new cells that were received. The cells used in this study were more round and cuboidal shaped compared to the new batch of cells, which were more elongated. The

old cells were smaller in size and were unable to attach and spread out on the surface, whereas the new cells were much larger in size. The morphology of the new cells were similar to the confocal microscope picture provided by the American Type Culture Collection datasheet. In addition, both cell sources were tested for cytotoxicity in our laboratory via an IL-8 ELISA after the conclusion of this study. There was an increase in IL-8 secretion in the old batch of cells which was not observed in the new cells. Therefore, confirmation of the results of our study is needed using both cell sources in future experiments.

5.5 Conclusion

In support of our hypothesis, we demonstrate that Cav1 binds with Notch2 and mediates the intracellular activation of ACE and EMT in human lung epithelial cells, through the modulation of activated Notch2 expression. Our findings unveil a novel role for Cav1 in the context of the MK-Notch2-ACE signaling pathway in EMT in human lung epithelial cells.

Previously, it was shown by our group and others that MK regulates downstream ACE expression leading to EMT. Our group showed that MK binds to the cell surface receptor Notch2 to upregulate ACE expression. However, since there is a lack of interaction between Notch2 and ACE, the signaling mechanism remains unclear. This study demonstrates that Cav1 binds specifically to Notch2 and is a key mediator of ACE signaling in lung epithelial cells (**Figure 14**).

This study provides insight into a novel signaling pathway that is induced by MK, a highly upregulated cytokine and growth factor in ARDS patients. Cav1 is an important mediator of the MK-Notch2 receptor complex which leads to downstream activation of ACE and EMT signaling. Our study suggests that Cav1 may be a potential target for the MK-induced ACE and EMT signaling in ARDS patients with pulmonary fibrosis.

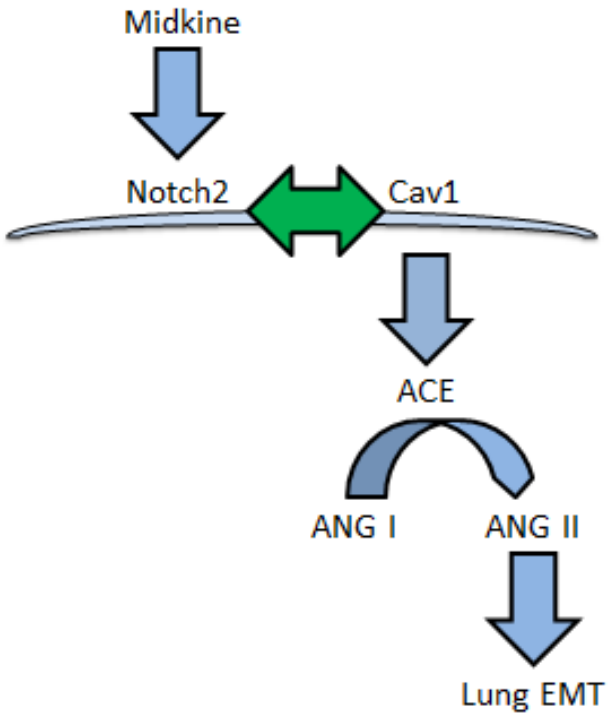

Figure 14. Proposed MK-Notch2-Cav1-ACE signaling pathway in human lung epithelial cells. This study demonstrates that Cav1 binds specifically with Notch2 and acts as a key mediator of ACE signaling in lung epithelial cells. Thus, Cav1 is a key mediator of the MK-Notch2-ACE signaling pathway in lung epithelial cells.

5-2 FUTURE DIRECTIONS

Since atypical EMT marker expression was observed in our experiments, it will be necessary to repeat the experiments using a new batch of lung epithelial cells. We must confirm our findings with the new cells we recently received in our laboratory.

In addition, we will repeat the experiments for Cav1 knockdown followed by rhMK stimulation in lung epithelial cells. Power analyses were performed for the Cav1 siRNA + MK group compared to the scrambled siRNA + MK group to determine the sample size required to detect differences between groups.

In our previous study, we demonstrated that MK levels are significantly upregulated in the plasma of ARDS patients within 24 hours of diagnosis. We have established an *in vitro* model using a two-hit stimulation of HCl and mechanical stretch to induce MK expression. In future experiments, we will detect MK expression in cell culture supernatant to determine whether stimulation with HCl and mechanical stretch may increase MK secretion in lung epithelial cells.

In this study, we demonstrated that rhMK stimulation of human lung epithelial cells led to an autocrine signaling mechanism which led to a high production of endogenous MK. However, there is a possibility that the high endogenous MK expression is attributed to rhMK still bound to the surface. In addition, it has been shown that different post-translational modifications of the MK protein may allow a longer or shorter half-life. In this case, future experiments could be carried out to verify endogenous MK expression using a different species of MK (instead of human) and use different host species of antibodies to detect MK expression on Western blot.

Alternatively, we could measure MK gene expression using quantitative polymerase chain reaction (q-PCR) to determine whether MK gene transcript levels are upregulated. Increased MK gene expression would confirm endogenous protein expression.

Our studies revealed a specific interaction of Cav1 with Notch2 in human lung epithelial cells. Notch2 expression was destabilized after Cav1 knockdown, suggesting a regulatory role of Cav1 on Notch2. To further investigate the relationship of Cav1 and Notch2, future studies will be conducted to establish the mechanism of Cav1 in regulating Notch2, as this is a novel interaction that deserves attention. In the future, it may be interesting to determine whether HCl or mechanical stretch can influence the binding of Cav1 and Notch2. Furthermore, we will perform direct binding assays to determine whether Cav1 and Notch2 bind through a direct interaction or if it is mediated by a protein complex. A commonly used direct binding assay is the affinity chromatography experiment, also known as the Gluathione S-Transferase pull-down assay. Alternatively, we could transfect cells with recombinant human Cav1 and recombinant human Notch2 to examine their interaction.

Cav1 is a transmembrane protein but it may be found at the plasma membrane or in the cytosol and is function-dependent. For example, cell-surface receptor localization may induce increased expression of Cav1 at the plasma membrane, but transcytosis could cause Cav1 invagination into the cytosol. In our two-hit *in vitro* model of HCl and mechanical stretch, we observed total Cav1 expression in whole cell lysates; however, it may be of interest to investigate Cav1 expression and activity in separate subcellular compartments. In future experiments, this may be achieved

by cell fractionation to determine Cav1 expression in the plasma membrane, cytoplasmic, and nuclear fractions in order to clearly establish Cav1 activity in our two-hit *in vitro* model.

Future studies could also focus on the phosphorylation of tyrosine-14, which may be activated upon mechanotransduction or mechanical stretch [154]. In our study, we determined total Cav1 expression in whole cell lysates; however, Cav1 phosphorylation may be induced upon stimulation with HCl, mechanical stretch, or rhMK. Thus, it may shed light on the molecular mechanism of Cav1 in regulating activated Notch2 cleavage, downstream ACE signaling, and EMT markers.

Through this study, we have established that Cav1 may play a key role in lung fibrosis by regulating ACE and mesenchymal marker expression *in vitro*. We used Cav1 siRNA to knock down Cav1 protein expression. Daidzein (an eNOS inhibitor) is a commercially available Cav1 blocker which may also be used to knock down Cav1 expression [155, 156]. Cav1 may be a potential target for MK-induced ACE and EMT signaling, and we could investigate this mechanism *in vivo* using delivery of Cav1 siRNA to mouse lungs or blocking Cav1 expression using Daidzein in an *in vivo* model of ARDS.

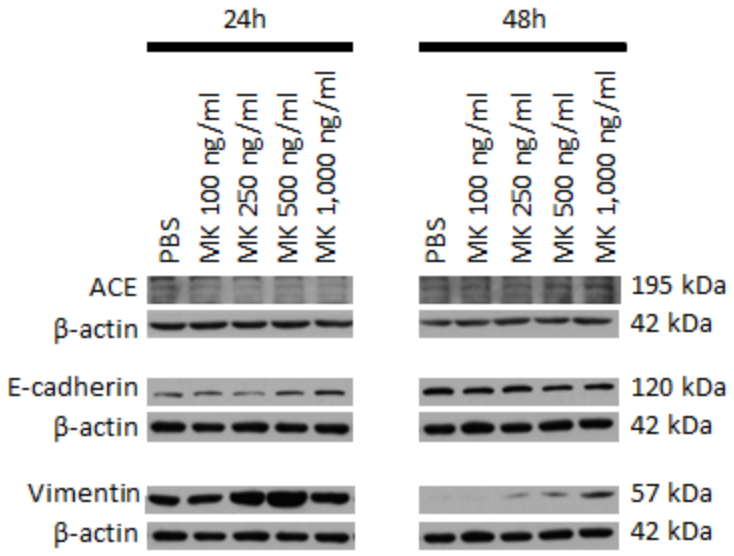

Supplementary Figure 1. Completed blots for optimization of rhMK stimulation of BEAS-2B cells shown in Figure 5. The completed set of Western blots for ACE, E-cadherin, and Vimentin protein expressions are shown above. The third group represents the dose of 250 ng/ml rhMK at 24 and 48h, which is not included in Figure 5 of the main thesis. β-actin was used as the loading control.

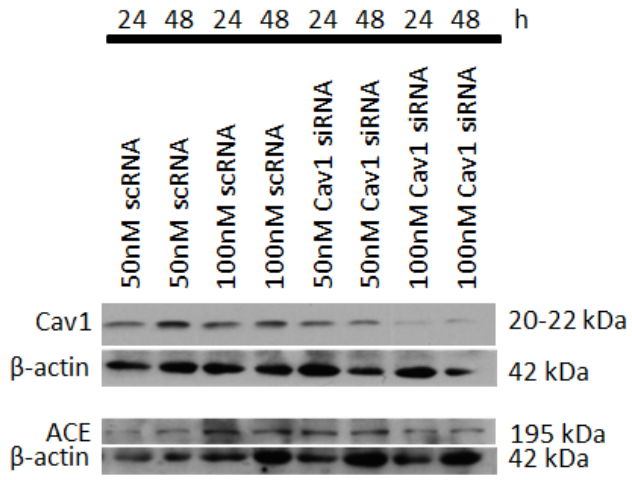

Supplementary Figure 2. Completed blots for optimization of Cav1 siRNA transfection of BEAS-2B cells shown in Figure 11. The completed set of Western blots for Cav1 and ACE protein expressions are shown above. The third, fourth, seventh, and eighth groups represent the dose of 100 nM siRNA at 24 and 48h, which are not included in Figure 11 of the main thesis. β-actin was used as the loading control.

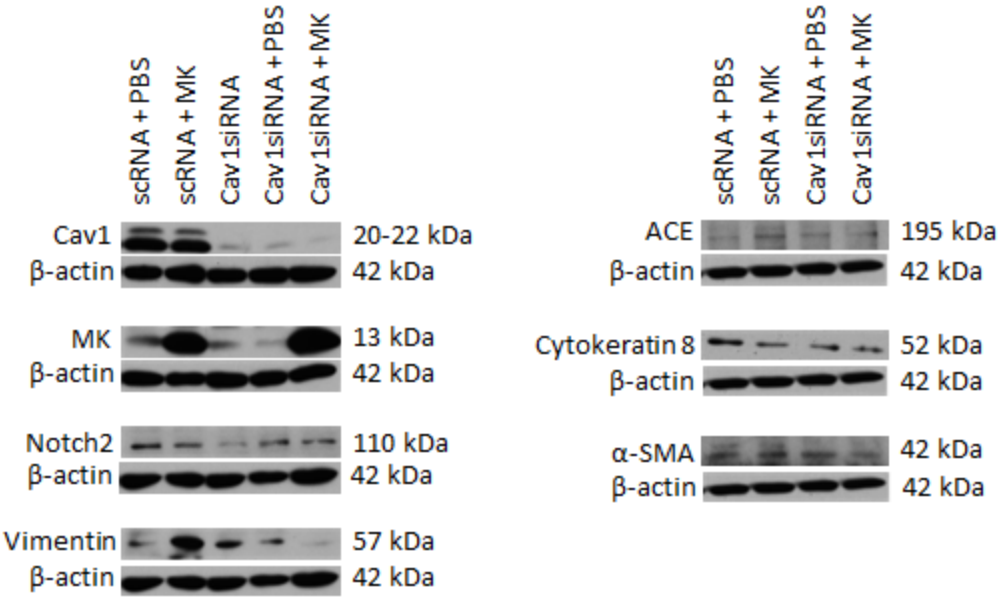

Supplementary Figure 3. Completed blots for Cav1 knockdown and rhMK stimulated BEAS-2B cells shown in Figure 13. The completed set of Western blots for Cav1, MK, Notch2, ACE, Cytokeratin8, α-SMA, and Vimentin protein expressions are shown above. The third group on the left panel represents the Cav1 siRNA transfected group alone, with no addition of PBS or rhMK, which is not included in Figure 13 of the main thesis. The right panel shows complete blots that were cut in the middle in Figure 13 for consistency with other the other blots on the left panel. β-actin was used as the loading control.

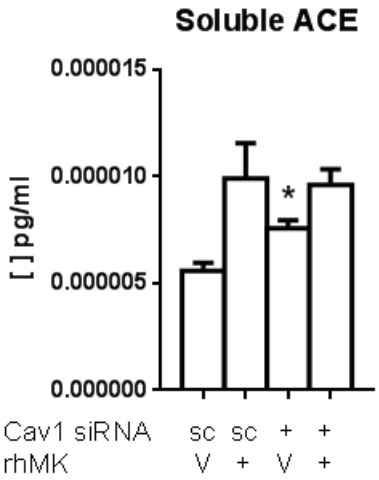

Supplementary Figure 4. Soluble ACE concentrations in cell culture supernatant detected by ELISA in the Cav1 siRNA + MK experiment shown in Figure 13. Cell culture supernatant (0.5 ml/well) from each group was collected following each Cav1 siRNA + MK experiment. The target concentration used for measuring supernatant was "very low target concentration" of < 156 pg/ml. Cell culture supernatant samples were undiluted. Experiments were performed 4 times in pooled triplicates. sc = Scrambled siRNA; + = Cav1 siRNA; V = Vehicle (PBS); + = Recombinant human MK (rhMK). * $p < 0.05$ vs. scRNA + V.

References

1. Force, T.A.D.T., *Acute respiratory distress syndrome: The Berlin Definition.* JAMA, 2012. **307**(23): p. 2526-33.
2. Zhang, R., et al., *Mechanical Stress and the Induction of Lung Fibrosis via the Midkine Signaling Pathway.* Am J Respir Crit Care Med, 2015. **192**(3): p. 315-23.
3. Cabrera-Benitez, N., et al., *Mechanical ventilation-associated lung fibrosis in acute respiratory distress syndrome.* Anesthesiology, 2014. **121**(1): p. 189-198.
4. Thompson, A.B., et al., *Immunological functions of the pulmonary epithelium.* Eur Respir J, 1995. **8**(1): p. 127-49.
5. Crystal, R.G., et al., *Airway epithelial cells: current concepts and challenges.* Proc Am Thorac Soc, 2008. **5**(7): p. 772-7.
6. Knight, D.A. and S.T. Holgate, *The airway epithelium: structural and functional properties in health and disease.* Respirology, 2003. **8**(4): p. 432-46.
7. Crapo, J.D., et al., *Cell number and cell characteristics of the normal human lung.* Am Rev Respir Dis, 1982. **126**(2): p. 332-7.
8. Mason, R.J., *Biology of alveolar type II cells.* Respirology, 2006. **11 Suppl**: p. S12-5.
9. Ashbaugh, D., et al., *Acute respiratory distress in adults.* Lancet, 1967. **2**(7511): p. 319-323.
10. Bernard, G., et al., *Report of the American-European Consensus Conference on Acute Respiratory Distress Syndrome: Definitions, mechanisms, relevant outcomes, and clinical trial coordination.* J Crit Care, 1994. **9**(1): p. 72-81.
11. Niederman, M.S. and A.M. Fein, *Sepsis syndrome, the adult respiratory distress syndrome, and nosocomial pneumonia. A common clinical sequence.* Clin Chest Med, 1990. **11**(4): p. 633-56.
12. Ware, L.B. and M.A. Matthay, *The acute respiratory distress syndrome.* N Engl J Med, 2000. **342**(18): p. 1334-49.
13. Marks, M., et al., *Managing malaria in the intensive care unit.* Br J Anaesth, 2014. **113**(6): p. 910-21.
14. Esteban, A., et al., *Evolution of mechanical ventilation in response to clinical research.* Am J Respir Crit Care Med, 2008. **177**(2): p. 170-7.
15. Rubenfeld, G., et al., *Incidence and outcomes of acute lung injury.* N Engl J Med, 2005. **353**: p. 1685-1693.
16. Lewandowski, K. and M. Lewandowski, *Epidemiology of ARDS.* Minerva Anesthesiol, 2006. **72**(6): p. 473-477.
17. Rubenfeld, G.D. and M.S. Herridge, *Epidemiology and outcomes of acute lung injury.* Chest, 2007. **131**(2): p. 554-62.
18. Masclans, J.R., et al., *Quality of life, pulmonary function, and tomographic scan abnormalities after ARDS.* Chest, 2011. **139**(6): p. 1340-6.
19. Pittet, J.F., et al., *Biological markers of acute lung injury: prognostic and pathogenetic significance.* Am J Respir Crit Care Med, 1997. **155**(4): p. 1187-205.

20. Bachofen, M. and E.R. Weibel, *Alterations of the gas exchange apparatus in adult respiratory insufficiency associated with septicemia.* Am Rev Respir Dis, 1977. **116**(4): p. 589-615.
21. Ware, L.B. and M.A. Matthay, *Alveolar fluid clearance is impaired in the majority of patients with acute lung injury and the acute respiratory distress syndrome.* Am J Respir Crit Care Med, 2001. **163**(6): p. 1376-83.
22. Matthay, M.A. and J.P. Wiener-Kronish, *Intact epithelial barrier function is critical for the resolution of alveolar edema in humans.* Am Rev Respir Dis, 1990. **142**(6 Pt 1): p. 1250-7.
23. Slutsky, A.S. and V.M. Ranieri, *Ventilator-induced lung injury.* N Engl J Med, 2013. **369**(22): p. 2126-36.
24. Marini, J.J., *Evolving concepts in the ventilatory management of acute respiratory distress syndrome.* Clin Chest Med, 1996. **17**(3): p. 555-75.
25. Gattinoni, L., et al., *Adult respiratory distress syndrome profiles by computed tomography.* J Thorac Imaging, 1986. **1**(3): p. 25-30.
26. Maunder, R.J., et al., *Preservation of normal lung regions in the adult respiratory distress syndrome. Analysis by computed tomography.* JAMA, 1986. **255**(18): p. 2463-5.
27. Network, T.A.R.D.S., *Ventilation with Lower Tidal Volumes as Compared with Traditional Tidal Volumes for Acute Lung Injury and the Acute Respiratory Distress Syndrome.* New England Journal of Medicine, 2000. **342**(18): p. 1301-1308.
28. Whitehead, T. and A.S. Slutsky, *The pulmonary physician in critical care * 7: ventilator induced lung injury.* Thorax, 2002. **57**(7): p. 635-42.
29. Madtes, D.K., et al., *Elevated transforming growth factor-alpha levels in bronchoalveolar lavage fluid of patients with acute respiratory distress syndrome.* Am J Respir Crit Care Med, 1998. **158**(2): p. 424-30.
30. Wynn, T.A., *Cellular and molecular mechanisms of fibrosis.* J Pathol, 2008. **214**(2): p. 199-210.
31. Martin, C., et al., *Pulmonary Fibrosis Correlates With Outcome in Adult Respiratory Distress Syndrome.* Chest, 1995. **107**(1): p. 196-200.
32. Cabrera-Benitez, N.E., et al., *Mechanical stress induces lung fibrosis by epithelial-mesenchymal transition.* Crit Care Med, 2012. **40**(2): p. 510-7.
33. Ichikado, K., et al., *Fibroproliferative changes on high-resolution CT in the acute respiratory distress syndrome predict mortality and ventilator dependency: a prospective observational cohort study.* BMJ Open, 2012. **2**(2): p. e000545.
34. Zapol, W.M., et al., *Pulmonary fibrosis in severe acute respiratory failure.* Am Rev Respir Dis, 1979. **119**(4): p. 547-54.
35. Papazian, L., et al., *A contributive result of open-lung biopsy improves survival in acute respiratory distress syndrome patients.* Crit Care Med, 2007. **35**(3): p. 755-62.
36. Tomashefski, J.F., Jr., et al., *The pulmonary vascular lesions of the adult respiratory distress syndrome.* Am J Pathol, 1983. **112**(1): p. 112-26.
37. Meduri, G.U., et al., *Corticosteroid rescue treatment of progressive fibroproliferation in late ARDS. Patterns of response and predictors of outcome.* Chest, 1994. **105**(5): p. 1516-27.
38. Hewitson, T.D., *Renal tubulointerstitial fibrosis: common but never simple.* Am J Physiol Renal Physiol, 2009. **296**(6): p. F1239-44.

39. Strutz, F. and M. Zeisberg, *Renal fibroblasts and myofibroblasts in chronic kidney disease.* J Am Soc Nephrol, 2006. **17**(11): p. 2992-8.
40. Grande, M.T. and J.M. Lopez-Novoa, *Fibroblast activation and myofibroblast generation in obstructive nephropathy.* Nat Rev Nephrol, 2009. **5**(6): p. 319-28.
41. Zeisberg, M. and J.S. Duffield, *Resolved: EMT produces fibroblasts in the kidney.* J Am Soc Nephrol, 2010. **21**(8): p. 1247-53.
42. Kanasaki, K., G. Taduri, and D. Koya, *Diabetic nephropathy: the role of inflammation in fibroblast activation and kidney fibrosis.* Front Endocrinol (Lausanne), 2013. **4**: p. 7.
43. Liu, Y., *Cellular and molecular mechanisms of renal fibrosis.* Nat Rev Nephrol, 2011. **7**(12): p. 684-96.
44. Kalluri, R. and E.G. Neilson, *Epithelial-mesenchymal transition and its implications for fibrosis.* Journal of Clinical Investigation, 2003. **112**(12): p. 1776-1784.
45. Hoyles, R.K., et al., *An essential role for resident fibroblasts in experimental lung fibrosis is defined by lineage-specific deletion of high-affinity type II transforming growth factor beta receptor.* Am J Respir Crit Care Med, 2011. **183**(2): p. 249-61.
46. Sargent, J.L., et al., *A TGFbeta-responsive gene signature is associated with a subset of diffuse scleroderma with increased disease severity.* J Invest Dermatol, 2010. **130**(3): p. 694-705.
47. Bellini, A. and S. Mattoli, *The role of the fibrocyte, a bone marrow-derived mesenchymal progenitor, in reactive and reparative fibroses.* Lab Invest, 2007. **87**(9): p. 858-70.
48. Bucala, R., et al., *Circulating fibrocytes define a new leukocyte subpopulation that mediates tissue repair.* Mol Med, 1994. **1**(1): p. 71-81.
49. Chesney, J., et al., *Regulated production of type I collagen and inflammatory cytokines by peripheral blood fibrocytes.* J Immunol, 1998. **160**(1): p. 419-25.
50. Pilling, D., et al., *Inhibition of fibrocyte differentiation by serum amyloid P.* J Immunol, 2003. **171**(10): p. 5537-46.
51. Abe, R., et al., *Peripheral blood fibrocytes: differentiation pathway and migration to wound sites.* J Immunol, 2001. **166**(12): p. 7556-62.
52. Quesnel, C., et al., *Alveolar fibrocyte percentage is an independent predictor of poor outcome in patients with acute lung injury.* Crit Care Med, 2012. **40**(1): p. 21-8.
53. Kalluri, R. and R.A. Weinberg, *The basics of epithelial-mesenchymal transition.* J Clin Invest, 2009. **119**(6): p. 1420-1428.
54. Kim, K.K., et al., *Alveolar epithelial cell mesenchymal transition develops in vivo during pulmonary fibrosis and is regulated by the extracellular matrix.* Proc Natl Acad Sci USA, 2006. **103**(35): p. 13180-5.
55. Mezzano, S., M. Ruiz-Ortega, and J. Egido, *Angiotensin II and renal fibrosis.* Hypertension, 2001. **38**: p. 635-638.
56. Chen, J., J.K. Chen, and R.C. Harris, *Angiotensin II induces epithelial-to-mesenchymal transition in renal epithelial cells through reactive oxygen species/Src/caveolin-mediated activation of an epidermal growth factor receptor-extracellular signal-regulated kinase signaling pathway.* Mol Cell Biol, 2012. **32**(5): p. 981-91.
57. Zhou, L. and Y. Liu, *Wnt/beta-catenin signaling and renin-angiotensin system in chronic kidney disease.* Curr Opin Nephrol Hypertens, 2016. **25**(2): p. 100-6.

58. Budinger, G.R.S., *Angiotensin II and pulmonary fibrosis, a new twist on an old story.* American Journal of Physiology - Lung Cellular and Molecular Physiology, 2011. **301**(3): p. L267-L268.
59. Muramatsu, T., *Midkine, a heparin-binding cytokine with multiple roles in development, repair and diseases.* Proc Jpn Acad Ser B Phys Biol Sci, 2010. **86**(4): p. 410-425.
60. Muramatsu, T. and K. Kadomatsu, *Midkine: An emerging target of drug development for treatment of multiple diseases.* Br J Pharmacol, 2014. **171**(4): p. 811-813.
61. Weckbach, L.T., T. Muramatsu, and B. Walzog, *Midkine in inflammation.* Sci World J, 2011. **11**: p. 2491-505.
62. Hobo, A., et al., *The growth factor midkine regulates the renin-angiotensin system in mice.* J Clin Invest, 2009. **119**(6): p. 1616-25.
63. Sato, W. and Y. Sato, *Midkine in nephrogenesis, hypertension, and kidney diseases.* Br J Pharmacol, 2014. **171**(4): p. 879-887.
64. Gungor, C., et al., *Notch signaling activated by replication stress-induced expression of midkine drives epithelial-mesenchymal transition and chemoresistance in pancreatic cancer.* Cancer Res, 2011. **71**(14): p. 5009-19.
65. Huang, Y., et al., *Midkine induces epithelial-mesenchymal transition through Notch2/Jak2-Stat3 signaling in human keratinocytes.* Cell Cycle, 2008. **7**(11): p. 1613-1622.
66. Kosugi, T. and W. Sato, *Midkine and the kidney: health and diseases.* Nephrol Dial Transplant, 2012. **27**(1): p. 16-21.
67. Zhang, H., et al., *PKC/midkine pathway drives hypoxia-induced proliferation and differentiation of human lung epithelial cells.* Am J Physiol Cell Physiol, 2014. **306**: p. C648-C658.
68. Muramatsu, H., et al., *LDL receptor-related protein as a component of the midkine receptor.* Biochem Biophys Res Commun, 2000. **270**(3): p. 936-41.
69. Muramatsu, H., et al., *a4B1- and a6B1- Integrins are functional receptors for midkine, a heparin-binding growth factor.* J Cell Sci, 2004. **117**(22): p. 5405-5415.
70. Stoica, G.E., et al., *Midkine binds to anaplastic lymphoma kinase (ALK) and acts as a growth factor for different cell types.* J Biol Chem, 2002. **277**(39): p. 35990-8.
71. Cohen, S., et al., *The cytokine midkine and its receptor RPTPzeta regulate B cell survival in a pathway induced by CD74.* J Immunol, 2012. **188**(1): p. 259-69.
72. Gungor, C., et al., *Midkine activates Notch signalling in PDAC.* Br J Pharmacol, 2014. **171**(4): p. 849-858.
73. Mohr, O.L., *Character changes caused by mutation of an entire region of a chromosome in Drosophila.* Genetics, 1919. **4**(3): p. 275-282.
74. High, F.A. and J.A. Epstein, *The multifaceted role of Notch in cardiac development and disease.* Nat Rev Genet, 2008. **9**(1): p. 49-61.
75. Boucher, J.M., et al., *A receptor-specific function for Notch2 in mediating vascular smooth muscle cell growth arrest through cyclin-dependent kinase inhibitor 1B.* Circ Res, 2013. **113**(8): p. 975-85.
76. Pancewicz, J. and C. Nicot, *Current views on the role of Notch signaling and the pathogenesis of human leukemia.* BMC Cancer, 2011. **11**: p. 502.

77. Kurooka, H., K. Kuroda, and T. Honjo, *Roles of the ankyrin repeats and C-terminal region of the mouse notch1 intracellular region.* Nucleic Acids Res, 1998. **26**(23): p. 5448-55.
78. Beatus, P., et al., *The origin of the ankyrin repeat region in Notch intracellular domains is critical for regulation of HES promoter activity.* Mech Dev, 2001. **104**(1-2): p. 3-20.
79. Aster, J.C., et al., *Essential Roles for Ankyrin Repeat and Transactivation Domains in Induction of T-Cell Leukemia by Notch1.* Molecular and Cellular Biology, 2000. **20**(20): p. 7505-7515.
80. Le Gall, M. and E. Giniger, *Identification of two binding regions for the suppressor of hairless protein within the intracellular domain of Drosophila notch.* J Biol Chem, 2004. **279**(28): p. 29418-26.
81. Kurooka, H. and T. Honjo, *Functional interaction between the mouse notch1 intracellular region and histone acetyltransferases PCAF and GCN5.* J Biol Chem, 2000. **275**(22): p. 17211-20.
82. Kiel, M.J., et al., *Whole-genome sequencing identifies recurrent somatic NOTCH2 mutations in splenic marginal zone lymphoma.* J Exp Med, 2012. **209**(9): p. 1553-65.
83. Kraman, M. and B. McCright, *Functional conservation of Notch1 and Notch2 intracellular domains.* FASEB J, 2005. **19**(10): p. 1311-1313.
84. Artavanis-Tsakonas, S., M.D. Rand, and R.J. Lake, *Notch signaling: Cell fate control and integration in development.* Science, 1999. **284**(5415): p. 770-776.
85. Timmerman, L.A., et al., *Notch promotes epithelial-mesenchymal transition during cardiac development and oncogenic transformation.* Genes Dev, 2004. **18**(1): p. 99-115.
86. Mitsiadis, T.A., et al., *Expression of Notch 1, 2 and 3 is regulated by epithelial-mesenchymal interactions and retinoic acid in the developing mouse tooth and associated with determination of ameloblast cell fate.* J Cell Biol, 1995. **130**(2): p. 407-18.
87. Espinoza, I., et al., *Notch signaling: targeting cancer stem cells and epithelial-to-mesenchymal transition.* Onco Targets Ther, 2013. **6**: p. 1249-59.
88. Dang, T., et al., *Chromosome 19 translocation, overexpression, of Notch3, and human lung cancer.* J Nat Cancer Inst, 2000. **92**(16): p. 1355-1357.
89. Rae, F., et al., *Novel association of a diverse range of genes with renal cell carcinoma as identified by differential display.* Int J Cancer, 2000. **88**: p. 726-732.
90. Miyamoto, Y., et al., *Notch mediates TGFα-induced changes in epithelial differentiation during pancreatic tumorigenesis.* Cancer Cell, 2003. **3**(6): p. 565-576.
91. Wang, Z., et al., *Acquisition of epithelial-mesenchymal transition phenotype of gemcitabine-resistant pancreatic cancer cells is linked with activation of the notch signaling pathway.* Cancer Res, 2009. **69**(6): p. 2400-7.
92. Blaumueller, C., et al., *Intracellular cleavage of Notch leads to a heterodimeric receptor on the plasma membrane.* Cell, 1999. **90**: p. 281-291.
93. Bray, S.J., *Notch signalling: a simple pathway becomes complex.* Nat Rev Mol Cell Biol, 2006. **7**(9): p. 678-89.
94. Hamada, Y., et al., *Mutation in ankyrin repeats of the mouse Notch2 gene induces early embryonic lethality.* Development, 1999. **126**(15): p. 3415-3424.
95. Bernstein, K.E., et al., *A modern understanding of the traditional and nontraditional biological functions of angiotensin-converting enzyme.* Pharmacol Rev, 2013. **65**(1): p. 1-46.

96. Bader, M. and D. Ganten, *Update on tissue renin-angiotensin systems.* J Mol Med (Berl), 2008. **86**(6): p. 615-21.
97. Dzau, V., *Tissue renin-angiotensin system: Physiologic and pharmacologic implications.* Circulation, 1988. **77**(6 Pt 2): p. I-1-3.
98. Ng, K.K.F. and J.R. Vane, *Conversion of Angiotensin I to Angiotensin II.* Nature, 1967. **216**(5117): p. 762-766.
99. Marshall, R.P., et al., *Angiotensin II and the fibroproliferative response to acute lung injury.* Am J Physiol Lung Cell Mol Physiol, 2004. **286**(1): p. L156-64.
100. Ruiz-Ortega, M., et al., *Angiotensin II: a key factor in the inflammatory and fibrotic response in kidney diseases.* Nephrol Dial Transplant, 2006. **21**(1): p. 16-20.
101. Lavoz, C., et al., *Angiotensin II contributes to renal fibrosis independently of Notch pathway activation.* PLoS ONE, 2012. **7**(7): p. e40490.
102. Gorin, A.B., et al., *Release of angiotensin converting enzyme by the lung after Pseudomonas bacteremia in sheep.* J Clin Invest, 1981. **68**(1): p. 163-170.
103. Idell, S., et al., *Angiotensin Converting Enzyme in Bronchoalveolar Lavage in ARDS.* Chest, 1987. **91**(1): p. 52-56.
104. Wang, S., et al., *Caveolin-1 regulates neural differentiation of rat bone mesenchymal stem cells into neurons by modulating Notch signaling.* Int J Dev Neurosci, 2013. **31**(1): p. 30-5.
105. Glenney Jr., J. and D. Soppet, *Sequence and expression of Caveolin, a protein component of caveolae plasma membrane domains phosphorylated on tyrosine in Rous sarcoma virus-transformed fibroblasts.* Proc Natl Acad Sci USA, 1992. **89**: p. 10517-10521.
106. Williams, T. and M. Lisanti, *Caveolin1 in oncogenic transformation, cancer, and metastasis.* Am J Physiol Cell Physiol, 2005. **288**: p. C494-C506.
107. Fujimoto, T., et al., *Isoforms of Caveolin1 and caveolar structure.* J Cell Sci, 2000. **113**: p. 3509-3517.
108. Liu, P., M. Rudick, and R.G. Anderson, *Multiple functions of caveolin-1.* J Biol Chem, 2002. **277**(44): p. 41295-8.
109. Jin, Y., et al., *Caveolin-1: a critical regulator of lung injury.* American Journal of Physiology - Lung Cellular and Molecular Physiology, 2011. **300**(2): p. L151-L160.
110. Razani, B., et al., *Caveolin-1 null mice are viable but show evidence of hyperproliferative and vascular abnormalities.* J Biol Chem, 2001. **276**(41): p. 38121-38.
111. Parolini, I., et al., *Expression of Caveolin1 is required for the transport of Caveolin2 to the plasma membrane.* J Biol Chem, 1999. **274**(36): p. 25718-25725.
112. Mora, R., et al., *Caveolin-2 localizes to the golgi complex but redistributes to plasma membrane, caveolae, and rafts when co-expressed with caveolin-1.* J Biol Chem, 1999. **274**(36): p. 25708-17.
113. Drab, M., et al., *Loss of caveolae, vascular dysfunction, and pulmonary defects in caveolin-1 gene-disrupted mice.* Science, 2001. **293**(5539): p. 2449-52.
114. Park, D., et al., *Caveolin1/3 double-knockout mice are viable, but lack both muscle and non-muscle caveolae, and develop a severe cardiomyopathic phenotype.* Am J Pathol, 2002. **160**(6): p. 2207-2217.
115. McNally, E.M., et al., *Caveolin-3 in muscular dystrophy.* Hum Mol Genet, 1998. **7**(5): p. 871-7.

116. Lal, H., et al., *Caveolin and beta1-integrin coordinate angiotensinogen expression in cardiac myocytes.* Int J Cardiol, 2013. **168**(1): p. 436-45.
117. Campos, L.S., et al., *Notch, epidermal growth factor receptor, and beta1-integrin pathways are coordinated in neural stem cells.* J Biol Chem, 2006. **281**(8): p. 5300-9.
118. Maniatis, N.A., et al., *Caveolins and lung function.* Adv Exp Med Biol, 2012. **729**: p. 157-79.
119. Maniatis, N.A., et al., *Role of caveolin-1 expression in the pathogenesis of pulmonary edema in ventilator-induced lung injury.* Pulm Circ, 2012. **2**(4): p. 452-60.
120. Shivshankar, P., et al., *Caveolin-1 deficiency protects from pulmonary fibrosis by modulating epithelial cell senescence in mice.* Am J Respir Cell Mol Biol, 2012. **47**(1): p. 28-36.
121. Le Saux, O., et al., *The role of caveolin-1 in pulmonary matrix remodeling and mechanical properties.* Am J Physiol Lung Cell Mol Physiol, 2008. **295**(6): p. L1007-17.
122. Hoetzel, A., et al., *Carbon monoxide prevents ventilator-induced lung injury via caveolin-1.* Crit Care Med, 2009. **37**(5): p. 1708-15.
123. Razani, B., et al., *Caveolin-1-deficient mice are lean, resistant to diet-induced obesity, and show hypertriglyceridemia with adipocyte abnormalities.* J Biol Chem, 2002. **277**(10): p. 8635-47.
124. Larue, L. and A. Bellacosa, *Epithelial-mesenchymal transition in development and cancer: role of phosphatidylinositol 3' kinase/AKT pathways.* Oncogene, 2005. **24**(50): p. 7443-54.
125. Rajjayabun, P.H., et al., *Caveolin-1 expression is associated with high-grade bladder cancer.* Urology, 2001. **58**(5): p. 811-4.
126. Fong, A., et al., *Expression of caveolin-1 and caveolin-2 in urothelial carcinoma of the urinary bladder correlates with tumor grade and squamous differentiation.* Am J Clin Pathol, 2003. **120**(1): p. 93-100.
127. Kato, K., et al., *Overexpression of caveolin-1 in esophageal squamous cell carcinoma correlates with lymph node metastasis and pathologic stage.* Cancer, 2002. **94**(4): p. 929-33.
128. Ito, Y., et al., *Caveolin-1 overexpression is an early event in the progression of papillary carcinoma of the thyroid.* Br J Cancer, 2002. **86**(6): p. 912-6.
129. Satoh, T., et al., *Caveolin-1 expression is a predictor of recurrence-free survival in pT2N0 prostate carcinoma diagnosed in Japanese patients.* Cancer, 2003. **97**(5): p. 1225-33.
130. Wiechen, K., et al., *Caveolin-1 is down-regulated in human ovarian carcinoma and acts as a candidate tumor suppressor gene.* Am J Pathol, 2001. **159**(5): p. 1635-43.
131. Engelman, J.A., et al., *Reciprocal regulation of neu tyrosine kinase activity and caveolin-1 protein expression in vitro and in vivo. Implications for human breast cancer.* J Biol Chem, 1998. **273**(32): p. 20448-55.
132. Fiucci, G., et al., *Caveolin-1 inhibits anchorage-independent growth, anoikis and invasiveness in MCF-7 human breast cancer cells.* Oncogene, 2002. **21**(15): p. 2365-75.
133. Sloan, E.K., K.L. Stanley, and R.L. Anderson, *Caveolin-1 inhibits breast cancer growth and metastasis.* Oncogene, 2004. **23**(47): p. 7893-7.
134. Razani, B., et al., *Caveolin-1 expression is down-regulated in cells transformed by the human papilloma virus in a p53-dependent manner. Replacement of caveolin-1*

expression suppresses HPV-mediated cell transformation. Biochemistry, 2000. **39**(45): p. 13916-24.
135. Yoo, S.H., et al., *Expression of caveolin-1 is associated with poor prognosis of patients with squamous cell carcinoma of the lung.* Lung Cancer, 2003. **42**(2): p. 195-202.
136. Yang, G., et al., *Elevated expression of caveolin is associated with prostate and breast cancer.* Clin Cancer Res, 1998. **4**(8): p. 1873-80.
137. Li, L., et al., *Caveolin-1 mediates testosterone-stimulated survival/clonal growth and promotes metastatic activities in prostate cancer cells.* Cancer Res, 2001. **61**(11): p. 4386-92.
138. Chanvorachote, P., V. Pongrakhananon, and P. Chunhacha, *Prolonged nitric oxide exposure enhances anoikis resistance and migration through epithelial-mesenchymal transition and caveolin-1 upregulation.* Biomed Res Int, 2014. **2014**: p. 941359.
139. Joo, H.J., et al., *Increased expression of caveolin-1 and microvessel density correlates with metastasis and poor prognosis in clear cell renal cell carcinoma.* BJU Int, 2004. **93**(3): p. 291-6.
140. Ho, C.C., et al., *Up-regulated caveolin-1 accentuates the metastasis capability of lung adenocarcinoma by inducing filopodia formation.* Am J Pathol, 2002. **161**(5): p. 1647-56.
141. Maniatis, N.A., et al., *Reduced expression of angiotensin I-converting enzyme in caveolin-1 knockout mouse lungs.* Microvasc Res, 2010. **80**(2): p. 250-7.
142. Uyy, E., et al., *Upregulation of caveolin-1 expression is associated with structural modifications of endothelial cells in diabetic lung.* Microvasc Res, 2010. **79**(2): p. 154-9.
143. Li, Y., et al., *Caveolin-1 promote astroglial differentiation of neural stem/progenitor cells through modulating Notch1/NICD and Hes1 expressions.* Biochem Biophys Res Commun, 2011. **407**(3): p. 517-24.
144. Raghavendran, K., et al., *Aspiration-induced lung injury.* Crit Care Med, 2011. **39**(4): p. 818-26.
145. Zhao, G., et al., *ERbeta-mediated estradiol enhances epithelial mesenchymal transition of lung adenocarcinoma through increasing transcription of midkine.* Mol Endocrinol, 2012. **26**(8): p. 1304-15.
146. Wu, C.H., et al., *Nickel-induced epithelial-mesenchymal transition by reactive oxygen species generation and E-cadherin promoter hypermethylation.* J Biol Chem, 2012. **287**(30): p. 25292-302.
147. Doerner, A.M. and B.L. Zuraw, *TGF-β1induced epithelial to mesenchymal transition (EMT) in human bronchial epithelial cells is enhanced by IL-1β but not abrogated by corticosteroids.* Respir Res, 2009. **10**(1): p. 1-15.
148. Hosper, N.A., et al., *Epithelial-to-mesenchymal transition in fibrosis: collagen type I expression is highly upregulated after EMT, but does not contribute to collagen deposition.* Exp Cell Res, 2013. **319**(19): p. 3000-9.
149. De Smedt, L., S. Palmans, and X. Sagaert, *Tumour budding in colorectal cancer: what do we know and what can we do?* Virchows Arch, 2016. **468**(4): p. 397-408.
150. Grigore, A.D., et al., *Tumor Budding: The Name is EMT. Partial EMT.* Journal of Clinical Medicine, 2016. **5**(5): p. 51.
151. Grosse-Wilde, A., et al., *Stemness of the hybrid Epithelial/Mesenchymal State in Breast Cancer and Its Association with Poor Survival.* PLoS ONE, 2015. **10**(5): p. e0126522.

152. Rawnaq, T., et al., *The Multifunctional Growth Factor Midkine Promotes Proliferation and Migration in Pancreatic Cancer.* Molecular Cancer Research, 2014. **12**(5): p. 670.
153. Novotny, W.F., et al., *Identification of novel heparin-releasable proteins, as well as the cytokines midkine and pleiotrophin, in human postheparin plasma.* Arterioscler Thromb, 1993. **13**(12): p. 1798-805.
154. Zhang, B., et al., *Caveolin-1 phosphorylation is required for stretch-induced EGFR and Akt activation in mesangial cells.* Cell Signal, 2007. **19**(8): p. 1690-700.
155. Sharma, S., M. Singh, and P. Sharma, *Ameliorative effect of daidzein: A Caveolin1 inhibitor in vascular endothelium dysfunction induced by ovariectomy.* Indian J Exp Biol, 2012. **50**: p. 28-34.
156. Woodman, O.L. and M. Boujaoude, *Chronic treatment of male rats with daidzein and 17β-oestradiol induces the contribution of EDHF to endothelium-dependent relaxation.* British Journal of Pharmacology, 2004. **141**(2): p. 322-328.

Appendix A

Caveolin1 siRNA SMARTpool target sequences. *Information provided by Dharmacon-Thermo Fisher Scientific (Waltham, MA, USA).*

ON-TARGETplus Human Caveolin1 siRNA SMARTpool	Target Sequence
ON-TARGETplus SMARTpool siRNA J-003467-06, CAV1	CUAAACACCUCAACGAUGA
ON-TARGETplus SMARTpool siRNA J-003467-07, CAV1	GCAAAUACGUAGACUCGGA
ON-TARGETplus SMARTpool siRNA J-003467-08, CAV1	GCAGUUGUACCAUGCAUUA
ON-TARGETplus SMARTpool siRNA J-003467-09, CAV1	GCAUCAACUUGCAGAAAGA

Copyright Acknowledgements

None.